

Prediction based on conditional distributions of vine copulas

Bo Chang* Harry Joe
 Department of Statistics
 University of British Columbia

July 22, 2018

Abstract

Vine copula models are a flexible tool in multivariate non-Gaussian distributions. For data from an observational study where the explanatory variables and response variables are measured over sampling units, we propose a vine copula regression method that uses regular vines and handles mixed continuous and discrete variables. This method can efficiently compute the conditional distribution of the response variable given the explanatory variables. Furthermore, we provide a theoretical analysis of the asymptotic conditional cumulative distribution function and quantile functions arising from vine copulas. Assuming all variables have been transformed to standard normal, the conditional quantile function could be asymptotically linear, sublinear, or constant with respect to the explanatory variables in different extreme directions, depending on the dependence properties of bivariate copulas in joint tails. The performance of the proposed method is evaluated on simulated data sets and a real data set. The experiments demonstrate that the vine copula regression method is superior to linear regression in making inferences with conditional heteroscedasticity.

Keywords: regression, nonlinear conditional mean, conditional quantiles, heteroscedasticity, boundary conditional distribution, tail order, Archimedean copula

1 Introduction

In the context of an observational study, i.e., the response variable y and the explanatory variables $\mathbf{x} = (x_1, \dots, x_p)$ are measured simultaneously, a natural approach is to fit a joint distribution to (x_1, \dots, x_p, y) assuming a random sample $(x_{i1}, \dots, x_{ip}, y_i)$ for $i = 1, \dots, n$, and then obtain the conditional distribution of y given \mathbf{x} for making predictions. For example, conditional expectation and conditional quantiles can be obtained from the conditional distribution for out-of-sample point estimates and prediction intervals. This becomes the usual multiple regression if the joint distribution of (\mathbf{x}, y) is multivariate Gaussian. Unlike multiple regression, this approach uses information on the distributions of the variables and does not specify a simple linear or polynomial equation for the conditional expectation. Polynomial equations can only be valid locally and generally have poor performance in the extremes of the predictor space.

To make this approach work, there are two major questions to be addressed: (A) *How to model the joint distribution of (x_1, \dots, x_p, y) ?* (B) *How to efficiently compute the conditional distribution of y given \mathbf{x} from a multivariate distribution?* For question (A), the vine copula or pair-copula construction is a flexible tool in high-dimensional dependence modeling; see Bedford and Cooke (2002), Aas et al. (2009), Brechmann et al. (2012), Dissmann et al. (2013), Joe (2014). The possibility of applying copulas for prediction and regression has been explored, but an algorithm is needed in general for (B) when some variables are continuous and others are discrete. Parsa and Klugman (2011) use a multivariate Gaussian copula to model the joint distribution, and conditional distributions have closed-form expressions. However, Gaussian copulas do not handle tail dependence or tail asymmetry, so can lead to incorrect inferences in the joint tails. Vine copulas are used by Kraus and Czado (2017) and Schallhorn et al. (2017) for quantile regression, but the vine

*Corresponding author: bchang@stat.ubc.ca. Department of Statistics, University of British Columbia, Vancouver, BC V6T 1Z4, Canada.

structure is restricted to a boundary class of vines called the D-vine. A general regular-vine (R-vine) copula is adopted in Cooke et al. (2015), for the case where the response variable and explanatory variables are continuous.

In this paper, we propose a method, called the vine copula regression, that uses R-vines and handles mixed continuous and discrete variables. That is, the predictor and response variables can be either continuous or discrete. As a result, we have a unified approach for regression and (ordinal) classification. This approach is interpretable, and various shapes of conditional quantiles of y as a function of \mathbf{x} can be obtained depending on how pair-copulas are chosen on the edges of the vine.

A contribution of the paper is a theoretical analysis of the asymptotic conditional cumulative distribution function (CDF) and quantile function for vine copula regression. This analysis sheds light on the advantage of vine copula regression methods: flexible asymptotic tail behavior. To easily compare with the Gaussian copula or linear regression equations when all variables have Gaussian distributions, we assume y and the components of \mathbf{x} have been transformed to standard normal $N(0, 1)$ variables y^* , \mathbf{x}^* . Leveraging the flexibility of bivariate copulas on the edges of the vine, the conditional quantile function of y^* could be asymptotically linear, sublinear, or constant with respect to the transformed explanatory variables \mathbf{x}^* , as components of \mathbf{x}^* go to $\pm\infty$.

The remainder of the paper is organized as follows. Section 2 gives an overview of vine copulas. Section 3 describes the model fitting procedure and the prediction algorithm given a fitted vine regression model. Section 4 provides theoretical results on how the choices of bivariate copulas in a vine affect the asymptotic tail behaviors of the conditional CDF and quantile function. Section 5 and 6 present a simulation study and applications of vine regression. Section 7 concludes the paper.

2 Vine copulas

In this section, we provide an overview of vine copulas. A d -dimensional copula C is a multivariate distribution on the unit hypercube $[0, 1]^d$, with all univariate margins being $U(0, 1)$. Sklar's theorem provides a decomposition of a d -dimensional distribution into two parts: the marginal distributions and the associated copula (Sklar, 1959). It states that for a d -dimensional random vector $\mathbf{Y} = (Y_1, Y_2, \dots, Y_d)'$ following a joint distribution F with the j th univariate margin F_j , the copula associated with F is a distribution function $C : [0, 1]^d \rightarrow [0, 1]$ with $U(0, 1)$ margins that satisfies

$$F(\mathbf{y}) = C(F_1(y_1), \dots, F_d(y_d)), \quad \mathbf{y} \in \mathbb{R}^d.$$

If F is a continuous d -variate distribution function, then the copula C is unique. Otherwise C is unique on the set $\text{Range}(F_1) \times \dots \times \text{Range}(F_d)$.

Vine copulas use bivariate copulas as the basic building blocks along with vine graphs to specify the dependence structure. Sections 2.1 and 2.2 briefly review some results for bivariate copulas and vine copulas that are used subsequently.

2.1 Bivariate distributions based on copulas

Consider a bivariate random vector (Y_1, Y_2) with joint CDF $F_{12}(y_1, y_2)$, marginal CDFs F_1, F_2 , and probability density function (PDF) $f_{12}(y_1, y_2)$. By Sklar's theorem, there exists a copula $C(u_1, u_2)$ such that $F_{12}(y_1, y_2) = C(F_1(y_1), F_2(y_2))$.

If $C(u_1, u_2)$ is absolutely continuous, then its density function is $c(u_1, u_2) = \partial^2 C(u_1, u_2) / \partial u_1 \partial u_2$. The set of conditional CDFs given $U_2 = u_2$ is: $C_{1|2}(u_1|u_2) := \mathbb{P}(U_1 \leq u_1 | U_2 = u_2) = \partial C(u_1, u_2) / \partial u_2$. The conditional quantile function $C_{1|2}^{-1}(\cdot|u_2)$ is the inverse function of $C_{1|2}(\cdot|u_2)$. The other set of conditional CDFs $C_{2|1}(\cdot|u_1)$ and quantile functions $C_{2|1}^{-1}(\cdot|u_1)$ can be defined in a similar fashion.

Let f_1, f_2 and f_{12} be the density functions of Y_1, Y_2 and (Y_1, Y_2) respectively, with respect to Lebesgue measure for continuous random variables or counting measure for discrete ones. Next is a result from Stöber et al. (2015) and Section 3.9.5 of Joe (2014). The joint density function f_{12} can be decomposed as follows,

$$f_{12}(y_1, y_2) = \tilde{c}(y_1, y_2) f_1(y_1) f_2(y_2), \tag{2.1}$$

where \tilde{c} is defined below. If Y_j is discrete, we define $F_j(y_j^-) := \mathbb{P}(Y_j < y_j) = \lim_{t \uparrow y_j} F_j(t)$.

- If both Y_1 and Y_2 are continuous random variables, then $\tilde{c}(y_1, y_2) := c(F_1(y_1), F_2(y_2))$.
- If Y_1 is a discrete random variable and Y_2 is continuous, then

$$f_{12}(y_1, y_2) = \frac{\partial}{\partial y_2} [F_{12}(y_1, y_2) - F_{12}(y_1^-, y_2)] = [C_{1|2}(F_1(y_1)|F_2(y_2)) - C_{1|2}(F_1(y_1^-)|F_2(y_2))] f_2(y_2).$$

In this case, $\tilde{c}(y_1, y_2) := [C_{1|2}(F_1(y_1)|F_2(y_2)) - C_{1|2}(F_1(y_1^-)|F_2(y_2))] / f_1(y_1)$.

- If Y_1 is a continuous random variable and Y_2 is discrete, then $\tilde{c}(y_1, y_2) := [C_{2|1}(F_2(y_2)|F_1(y_1)) - C_{2|1}(F_2(y_2)|F_1(y_1^-))] / f_2(y_2)$.
- If both Y_1 and Y_2 are discrete random variables, then the density of (Y_1, Y_2) is:

$$f_{12}(y_1, y_2) = C(F_1(y_1), F_2(y_2)) - C(F_1(y_1^-), F_2(y_2)) - C(F_1(y_1), F_2(y_2^-)) + C(F_1(y_1^-), F_2(y_2^-)).$$

In this case,

$$\tilde{c}(y_1, y_2) := [C(F_1(y_1), F_2(y_2)) - C(F_1(y_1^-), F_2(y_2)) - C(F_1(y_1), F_2(y_2^-)) + C(F_1(y_1^-), F_2(y_2^-))] / [f_1(y_1)f_2(y_2)].$$

Tail order, denoted by κ , and as studied in Hua and Joe (2011), can be used as a measure of the strength of dependence in the joint tails of a copula. For bivariate copulas with positive dependence, the tail order has value between 1 and 2, with larger values indicating less dependence in the joint tail. The tail order can be larger than the dimension for negative dependence.

If there exists $\kappa_L > 0$ and some $\ell(u)$ that is slowly varying at 0^+ (i.e., $\ell(tu)/\ell(u) \sim 1$ as $u \rightarrow 0^+$ for all $t > 0$) such that $C(u, u) \sim u^{\kappa_L} \ell(u)$, as $u \rightarrow 0^+$, then κ_L is called the *lower tail order* of C and $\Upsilon_L = \lim_{u \rightarrow 0^+} \ell(u)$ is the lower tail order parameter. By reflection, the *upper tail order* is defined as κ_U such that $\bar{C}(1-u, 1-u) \sim u^{\kappa_U} \ell^*(u)$, as $u \rightarrow 0^+$, for some slowly varying function $\ell^*(u)$, where \bar{C} is the survival function of the copula C . The upper tail order parameter is then $\Upsilon_U = \lim_{u \rightarrow 0^+} \ell^*(u)$.

With $\kappa = \kappa_L$ or κ_U and $\Upsilon = \Upsilon_L$ or Υ_U , we further classify the tail property of a copula into the following:

- *Strong tail dependence*: $\kappa = 1$ with $\Upsilon > 0$.
- *Intermediate tail dependence*: $1 < \kappa < 2$, or $\kappa = 1$ and $\Upsilon = 0$.
- *Tail quadrant independence*: $\kappa = 2$ and the slowly varying function is (asymptotically) a constant.

2.2 Vine structures

A regular vine (R-vine) in d variables is a nested set of $d-1$ trees where the edges in the first tree are the nodes of the second tree, the edges of the second tree are the nodes of the third tree, etc. Vines and truncated vines provide a flexible approach to summarizing dependence in a multivariate distribution with edges in the first tree representing pairwise dependence and edges in subsequent trees representing conditional dependence. Vines extend Markov trees to allow for conditional dependence. A multivariate Gaussian distribution can be represented through vines when parameters on the edges of the vine are correlations in the first tree and partial correlations in subsequent trees; for tree ℓ ($2 \leq \ell < d$), the partial correlations are conditioned on $\ell-1$ variables.

In general, the first tree represents d variables as nodes and bivariate dependence of $d-1$ pairs of variables as edges. The second tree represents conditional dependence of $d-2$ pairs of variables conditioning on another variable; nodes are the edges in tree 1, and a pair of nodes could be connected if there is a common variable in the pair. The third tree represents conditional dependence of $d-3$ pairs of variables conditioning on two other variables; nodes are the edges in tree 2, and a pair of nodes could be connected if there are two common conditioning variables in the pair. This continues until tree $d-1$ has one edge that represents the conditional dependence of two variables conditioning on the remaining $d-2$ variables.

A formal definition, from Bedford and Cooke (2002), is as follows.

Definition 2.1. (Regular vine) \mathcal{V} is a regular vine on d elements, with $E(\mathcal{V}) = \bigcup_{i=1}^{d-1} E(T_i)$ denoting the set of edges of \mathcal{V} , if

1. $\mathcal{V} = (T_1, \dots, T_{d-1})$ [consists of $d - 1$ trees];
2. T_1 is a connected tree with nodes $N(T_1) = \{1, 2, \dots, d\}$, and edges $E(T_1)$, T_ℓ is a tree with nodes $N(T_\ell) = E(T_{\ell-1})$ [edges in a tree becomes nodes in the next tree];
3. (proximity) for $\ell = 2, \dots, d - 1$, for $\{n_1, n_2\} \in E(T_\ell)$, $\#(n_1 \Delta n_2) = 2$, where Δ denotes symmetric difference and $\#$ denotes cardinality [nodes joined in an edge differ by two elements].

To get a vine copula or pair-copula construction, for each edge $[jk|S] \in E(\mathcal{V})$ in the vine, there is a bivariate copula $C_{jk;S}$ associated with it. Let $\tilde{c}_{jk;S}(\cdot; \mathbf{y}_S)$ be as defined in Section 2.1 for $C_{jk;S}(\cdot; \mathbf{y}_S)$ when the conditioning value is \mathbf{y}_S , and let $C_{j|k;S}(a|b; \mathbf{y}_S) = \partial C_{jk;S}(a, b; \mathbf{y}_S) / \partial b$ and $C_{k|j;S}(b|a; \mathbf{y}_S) = \partial C_{jk;S}(a, b; \mathbf{y}_S) / \partial a$. The joint density of (Y_1, \dots, Y_d) can be decomposed according to the vine structure \mathcal{V} .

$$f_{1:d}(y_1, \dots, y_d) = \prod_{i=1}^d f_i(y_i) \cdot \prod_{[jk|S] \in E(\mathcal{V})} \tilde{c}_{jk;S}(y_j, y_k; \mathbf{y}_S). \quad (2.2)$$

The above representation for the case of absolutely continuous random variables is derived in Bedford and Cooke (2001); its extension to include some discrete variables is in Section 3.9.5 of Joe (2014). For simplicity of notation, we denote $F_{j|S}^+ = F_{j|S}(y_j | \mathbf{y}_S)$ and $F_{j|S}^- = \lim_{t \uparrow y_j} F_{j|S}(t | \mathbf{y}_S)$. If it is assumed that the copulas on edges of trees 2 to $d - 1$ do not depend on the values of the conditioning values, then $c_{jk;S}$ and $\tilde{c}_{jk;S}$ in (2.2) do not depend on \mathbf{y}_S ; i.e., $c_{jk;S}(\cdot) = c_{jk;S}(\cdot; \mathbf{y}_S)$ and $\tilde{c}_{jk;S}(\cdot) = \tilde{c}_{jk;S}(\cdot; \mathbf{y}_S)$. This is called the *simplifying assumption*. With the simplifying assumption, we have the following definition of $\tilde{c}_{jk;S}$.

- If Y_j and Y_k are both continuous, then $\tilde{c}_{jk;S}(y_j, y_k) := c_{jk;S}(F_{j|S}^+, F_{k|S}^+)$;
- If Y_j is continuous and Y_k is discrete, then

$$\tilde{c}_{jk;S}(y_1, y_k) := [C_{k|j;S}(F_{k|S}^+ | F_{j|S}^+) - C_{k|j;S}(F_{k|S}^- | F_{j|S}^+)] / f_{k|S}(y_k | \mathbf{y}_S);$$

- If Y_j is discrete and Y_k is continuous, then

$$\tilde{c}_{jk;S}(y_j, y_k) := [C_{j|k;S}(F_{j|S}^+ | F_{k|S}^+) - C_{j|k;S}(F_{j|S}^- | F_{k|S}^+)] / f_{j|S}(y_j | \mathbf{y}_S);$$

- If Y_j and Y_k are both discrete, then

$$\tilde{c}_{jk;S}(y_j, y_k) := [C_{jk;S}(F_{j|S}^+, F_{k|S}^+) - C_{jk;S}(F_{j|S}^-, F_{k|S}^+) - C_{jk;S}(F_{j|S}^+, F_{k|S}^-) + C_{jk;S}(F_{j|S}^-, F_{k|S}^-)] / [f_{j|S}(y_j | \mathbf{y}_S) f_{k|S}(y_k | \mathbf{y}_S)].$$

A t -truncated vine copula results if the copulas for trees T_{t+1}, \dots, T_{d-1} are all independence copulas, representing conditional independencies.

3 Vine copula regression

Consider the data structure for multiple regression with p explanatory variables x_1, \dots, x_p and response variable y as a sample of size n ; the data are $(x_{i1}, \dots, x_{ip}, y_i)$ for $i = 1, \dots, n$, considered as independent realizations of a random vector (X_1, \dots, X_p, Y) . If these data are considered as a sample in an observational study, then a natural approach is to fit a joint multivariate density to the variables x_1, \dots, x_p, y . This can be done using a flexible, parametric vine copula.

Researchers have applied D-vine copulas to quantile regressions (Kraus and Czado, 2017; Schallhorn et al., 2017). Their approach is to sequentially constructs a D-vine: it first links the predictor with the strongest dependence to y ; then a second variable with strongest conditional dependence to y given first predictor;

this procedure continues until an information criterion stop improving. This structure learning algorithm is similar to the forward selection in multiple regression and easiest to handle with a D-vine. However, it is known that forward selection does not usually produce an optimal solution. Compared to the existing D-vine-based methods, our proposed algorithm uses R-vines and is more flexible.

Furthermore, Schallhorn et al. (2017) propose a method based on continuous convolution to handle discrete variables, and estimate the vine copula non-parametrically. When variables are all monotonically related, the parametric approach that we are using can be simpler for interpretations and check monotonicity of conditional quantiles.

The remainder of this section is organized as follows. Section 3.1 introduces the model fitting and assessment procedure. Section 3.2 describes an algorithm that calculates the conditional CDF of the response variable of a new observation, given a fitted vine copula regression model. The conditional CDF can be further used to calculate the conditional mean and quantile for regression problems, and conditional probability mass function (PMF) for classification problems.

3.1 Model fitting and assessment

Due to the decomposition of a joint distribution to univariate marginal distributions and a dependence structure among variables, a two-stage estimation procedure can be adopted. Suppose the observed data are $(z_{i1}, z_{i2}, \dots, z_{id}) = (x_{i1}, \dots, x_{ip}, y_i)$, for $i = 1, \dots, n$ with $d = p + 1$.

1. Estimate the univariate marginal distributions \hat{F}_j , for $j = 1, \dots, d$, using parametric or non-parametric methods. The corresponding u-scores are obtained by applying the probability integral transform: $\hat{u}_{ij} = \hat{F}_j(z_{ij})$.
2. Fit a vine copula on the u-scores. There are two components: vine structure and bivariate copulas. Section 3.1.1 discusses how to choose a vine structure, and Section 3.1.2 presents a bivariate copula selection procedure.
3. Compute some conditional quantiles, with some predictors fixed and others varying, to check if the monotonicity properties are interpretable.

3.1.1 Vine structure learning

In this section, we introduce methods for learning or choosing truncated R-vine structures. From Kurowicka and Joe (2011), the total number of (untruncated) R-vines in d variables is $2^{(d-3)(d-2)}(d!/2)$. When the dimension d is small, it is possible to enumerate all $2^{(d-3)(d-2)}(d!/2)$ vines and find the best ℓ -truncated R-vine based on some objective functions such as those in Section 6.17 of Joe (2014). However, this is only feasible for $d \leq 8$ in practice. Greedy algorithms (Dissmann et al., 2013) and metaheuristic algorithms (Brechmann and Joe, 2014) are commonly adopted to find a locally optimal ℓ -truncated vine. The development of vine structure learning algorithms is an active research topic; various algorithms are proposed based on different heuristics. However, no heuristic method can be expected to be universally the best.

The goal of vine copula regression is to find the conditional distribution of the response variable, given the explanatory variables. In general, to calculate the conditional distribution from the joint distribution specified by a vine copula, computationally intensive multidimensional numerical integration is required. This could be avoided if we enforce a constraint on the vine structure such that the node containing the response variable as a conditioned variable is always a leaf node in T_ℓ , $\ell = 1, \dots, d - 1$. When this constraint is satisfied, Algorithm 3.1 computes the conditional CDF without numerical integration.

To construct a truncated R-vine that satisfies the constraint, we can first find a locally optimal t -truncated R-vine using the explanatory variables x_1, \dots, x_p . Then from level 1 to level t , the response variable y is sequentially linked to the node that satisfies the proximity condition and has the largest absolute (normal scores) correlation with y . Figure 1 demonstrates how to add a response variable to the R-vine of the explanatory variables, after each variables has been transformed to standard normal $N(0, 1)$. Given a 2-truncated R-vine $\mathcal{V} = (T_1, T_2)$ with $N(T_1) = \{1, \dots, 5\}$, $E(T_1) = N(T_2) = \{[12], [23], [24], [35]\}$, $E(T_2) = \{[13|2], [25|3], [34|2]\}$. Suppose the response variable is denoted by 6. The first step is to find the node that has the largest absolute correlation, i.e. $\arg \max_{1 \leq i \leq 6} |\rho_{i6}|$. Assume ρ_{36} is the largest, then node 3 and node

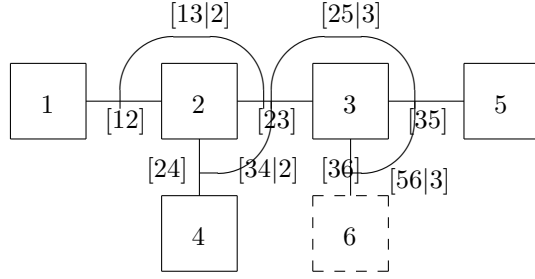


Figure 1: Adding a response variable to the R-vine of the explanatory variables. In this example, variables 1 to 5 represent the explanatory variables and variable 6 represents the response variable.

6 are linked: $N(T'_1) = N(T_1) \cup \{6\}$, $E(T'_1) = E(T_1) \cup \{[36]\}$. At level 2, according to the proximity condition, node [36] can be linked to either [23] or [35]. So we compare $\rho_{26;3}$ with $\rho_{56;3}$. If we assume $|\rho_{56;3}| > |\rho_{26;3}|$, then $E(T'_2) = E(T_2) \cup \{[56|3]\}$. So the new 2-truncated R-vine is $\mathcal{V}' = (T'_1, T'_2)$.

3.1.2 Bivariate copula selection

After fitting the univariate margins and deciding on the vine structure, parametric bivariate copulas can be fitted sequentially from tree 1, tree 2, etc. The results in Section 4 can provide guidelines of choices of bivariate copula families in order to match the expected behavior of conditional quantile functions in the extremes of the predictor space. With the simplifying assumption and parametric copula families, the log-likelihood of the bivariate copula $C_{j,k;S}$ on edge $[jk|S] \in E(\mathcal{V})$, is

$$\ell_{jk;S}(\boldsymbol{\theta}_{jk}) = \sum_{i=1}^n \log(\tilde{c}_{jk;S}(z_{ij}, z_{ik}; \boldsymbol{\theta}_{jk})).$$

Commonly used model selection criteria include Akaike information criterion (AIC) and Bayesian information criterion (BIC):

$$\text{AIC}_{jk;S}(\boldsymbol{\theta}_{jk}) = -2\ell_{jk;S}(\boldsymbol{\theta}_{jk}) + 2|\boldsymbol{\theta}_{jk}|, \quad \text{BIC}_{jk;S}(\boldsymbol{\theta}_{jk}) = -2\ell_{jk;S}(\boldsymbol{\theta}_{jk}) + \log(n)|\boldsymbol{\theta}_{jk}|,$$

where $|\boldsymbol{\theta}_{jk}|$ refers to the number of copula parameters in $c_{jk;S}$. For each candidate bivariate copula family on an edge, we first find the parameters that maximize the log-likelihood $\hat{\boldsymbol{\theta}}_{\text{MLE}}$. Then the copula family with the lowest AIC or BIC is selected.

3.2 Prediction

This section describes how to predict the conditional distribution of the response variable of a new observation, given a fitted vine copula regression model. We first present an algorithm that computes the conditional CDF of the response variable. If the response variable is continuous, the conditional quantile and mean can be calculated by inverting the conditional CDF and integrating the quantile function. If the response variable is discrete, the conditional PMF can be easily derived from the conditional CDF via finite difference.

Based on ideas of the algorithms in Chapter 6 of Joe (2014), Algorithm 3.1 can be applied to an R-vine with mixed continuous and discrete variables. The idea is that, given the structural constraint on the vine structure described in Section 3.1.1, conditional distributions are sequentially computed according to the vine structure, and the conditional distribution of the response variable given all the explanatory variables is obtained in the end. The input is a vine copula regression model with a vine array $A = (a_{kj})$, a vector of new explanatory variables $\mathbf{x} = (x_1, \dots, x_d)'$, and a percentile $u \in (0, 1)$. The vine array is an efficient and compact way to represent a vine structure; see Appendix A or Kurowicka and Joe (2011) or Joe (2014). The algorithm returns the conditional CDF of the response variable given the explanatory variables evaluated at u , that is, $p(u|\mathbf{x}) := \mathbb{P}(F_Y(Y) \leq u | \mathbf{X} = \mathbf{x})$. It calculates the conditional distributions $C_{j|a_{\ell j}; a_{1j}, \dots, a_{\ell-1, j}}$ and

$C_{a_{\ell j}|j;a_{1j},\dots,a_{\ell-1,j}}$ for $\ell = 1, \dots, n_{\text{trunc}}$ and $j = \ell + 1, \dots, d$, where n_{trunc} is the truncation level of the vine copula. For discrete variables, both the left-sided and right-sided limits of the conditional CDF are retained. In the end, $C_{d|a_{d-1,d};a_{1d},\dots,a_{d-2,d}}$ is returned.

If the response variable Y is continuous, then the conditional mean and conditional quantile can be calculated using $p(\cdot|\mathbf{x})$: the α -quantile is $F_Y^{-1}(p^{-1}(\alpha|\mathbf{x}))$, and the conditional mean is

$$E(Y|\mathbf{X} = \mathbf{x}) = \int_0^1 F_Y^{-1}(p^{-1}(\alpha|\mathbf{x}))d\alpha,$$

where $p^{-1}(\cdot|\mathbf{x})$ is calculated using the secant method, and the numerical integration is calculated using Monte Carlo methods or numerical quadrature. If the response variable Y is ordinal, then it is a classification problem; we only need to focus on the support of Y . The conditional CDF is fully specified by $p(F_Y(y)) = \mathbb{P}(Y \leq y|\mathbf{X} = \mathbf{x})$, where $y \in \{k : \mathbb{P}(Y = k) > 0\}$.

If the response variable Y is nominal, then the proposed method does not apply. An alternative vine-copula-based method is to fit a vine copula model for each class separately and use the Bayes' theorem to predict the class label. Specifically, for samples in class $Y = k$, we fit a vine copula density $\hat{f}_{\mathbf{X}|Y}(\mathbf{x}|k)$. Let $\hat{\pi}_k$ be the proportion of samples in class k in the training set. According the Bayes' theorem, the predicted probability that a sample belongs to class k is

$$\hat{f}_{Y|\mathbf{X}}(k|\mathbf{x}) = \frac{\hat{\pi}_k \hat{f}_{\mathbf{X}|Y}(\mathbf{x}|k)}{\sum_j \hat{\pi}_j \hat{f}_{\mathbf{X}|Y}(\mathbf{x}|j)}.$$

Since the distribution of predictors is modeled separately for each class, this alternative method is more flexible but has a high computational cost, especially when the number of classes is large.

4 Theoretical results on shapes of conditional quantile functions

From the properties of the multivariate normal distribution, if (X_1, \dots, X_p, Y) follows a multivariate normal distribution, then the conditional quantile function of $Y|X_1, \dots, X_p$ has the linear form

$$F_{Y|X_1, \dots, X_p}^{-1}(\alpha|x_1, \dots, x_p) = \beta_1 x_1 + \dots + \beta_p x_p + \Phi^{-1}(\alpha) \sqrt{1 - R_{Y;X_1, \dots, X_p}^2}, \quad 0 < \alpha < 1,$$

where $R_{Y;X_1, \dots, X_p}^2$ is the multiple correlation coefficient. Going beyond the normal distribution, we address the following question in this section: how does the choice of bivariate copulas in a vine copula regression model affect the conditional quantile function, especially when the explanatory variables are large (in absolute value)? For comparisons with multivariate normal, we assume the variables X_1, \dots, X_p, Y have been transformed so that they have marginal $N(0, 1)$ distributions. In this case, plots from vine copulas with one or two explanatory variables can show conditional quantile functions that are close to linear in the middle, and asymptotically linear, sublinear or constant along different directions to $\pm\infty$; Bernard and Czado (2015) have several figures show this pattern for the case of one explanatory variable. Such behavior cannot be obtained with regression equations that are linear in β 's and is hard to obtain with nonlinear regression functions that are directly specified.

We start with the bivariate case (one explanatory variable) in Section 4.1. Conditions are obtained to classify the asymptotic behavior of conditional quantile function into four categories: *strong linear*, *weak linear*, *sublinear* and *asymptotic constant*. For bivariate Archimedean copulas, the conditions are related to conditions on the Laplace transform generator. Section 4.2 studies the trivariate case $F_{Y|X_1, X_2}^{-1}(\alpha|x_1, x_2)$ with a trivariate vine copula. However, extending from bivariate to trivariate is challenging: the asymptotic conditional quantile depends on the direction in which (x_1, x_2) go to infinity. Section 4.2.1 analyzes the strongest possible dependence in the trivariate case: functional relationship between Y and (X_1, X_2) . It is difficult if not impossible to obtain a general result, given the marginal distribution of Y does not have a closed-form expression in general. We focus on a special case where the marginal distribution of Y can be calculated. It is shown that the conditional quantile function is asymptotically linear in x_1 or x_2 along a ray on the (x_1, x_2) -plane, and this is an extension of the bivariate strong linear case. Section 4.2.2 and 4.2.3

Algorithm 3.1 Conditional CDF of the response variable given the explanatory variables with which to predict; based on steps from Algorithms 4, 7, 17, 18 in Joe (2014).

1: Input: vine array $A = (a_{kj})$ with $a_{jj} = j$ for $j = 1, \dots, d$ on the diagonal. $\mathbf{u}^+ = (u_1^+, \dots, u_d^+)$, $\mathbf{u}^- = (u_1^-, \dots, u_d^-)$, where $u_j^+ = F_j(x_j)$ and $u_j^- = F_j(x_j^-)$ for $1 \leq j \leq d-1$, $u_d^+ = u_d^- \in [0, 1]$.

2: Output: $\mathbb{P}(F_d(X_d) \leq u_d^+ | X_1 = x_1, \dots, X_{d-1} = x_{d-1})$.

3: Compute $M = (m_{kj})$ in the upper triangle, where $m_{kj} = \max\{a_{1j}, \dots, a_{kj}\}$ for $k = 1, \dots, j-1$, $j = 2, \dots, d$.

4: Compute the $I = (I_{kj})$ indicator array as in Algorithm 5 in Joe (2014).

5: $s_j^+ = u_{a_{1j}}^+$, $s_j^- = u_{a_{1j}}^-$, $w_j^+ = u_j^+$, $w_j^- = u_j^-$, for $j = 1, \dots, d$.

6: **for** $\ell = 2, \dots, n_{\text{trunc}}$ **do**

7: **for** $j = \ell, \dots, d$ **do**

8: **if** $I_{\ell-1,j} = 1$ **then**

9: **if** $\text{isDiscrete}(j)$ **then**

10: $v_j'^+ \leftarrow \frac{C_{a_{\ell-1,j}; a_{1j} \dots a_{\ell-2,j}}(s_j^+, w_j^+) - C_{a_{\ell-1,j}; a_{1j} \dots a_{\ell-2,j}}(s_j^+, w_j^-)}{w_j^+ - w_j^-}$,

11: $v_j'^- \leftarrow \frac{C_{a_{\ell-1,j}; a_{1j} \dots a_{\ell-2,j}}(s_j^-, w_j^+) - C_{a_{\ell-1,j}; a_{1j} \dots a_{\ell-2,j}}(s_j^-, w_j^-)}{w_j^+ - w_j^-}$,

12: **else**

13: $v_j'^+ \leftarrow C_{a_{\ell-1,j}; a_{1j} \dots a_{\ell-2,j}}(s_j^+ | w_j^+)$,

14: $v_j'^- \leftarrow C_{a_{\ell-1,j}; a_{1j} \dots a_{\ell-2,j}}(s_j^- | w_j^+)$,

15: **end if**

16: **end if**

17: **if** $\text{isDiscrete}(a_{\ell-1,j})$ **then**

18: $v_j^+ \leftarrow \frac{C_{a_{\ell-1,j}; a_{1j} \dots a_{\ell-2,j}}(s_j^+, w_j^+) - C_{a_{\ell-1,j}; a_{1j} \dots a_{\ell-2,j}}(s_j^-, w_j^+)}{s_j^+ - s_j^-}$,

19: $v_j^- \leftarrow \frac{C_{a_{\ell-1,j}; a_{1j} \dots a_{\ell-2,j}}(s_j^+, w_j^-) - C_{a_{\ell-1,j}; a_{1j} \dots a_{\ell-2,j}}(s_j^-, w_j^-)}{s_j^+ - s_j^-}$,

20: **else**

21: $v_j^+ \leftarrow C_{j|a_{\ell-1,j}; a_{1j} \dots a_{\ell-2,j}}(w_j^+ | s_j^+)$, $v_j^- \leftarrow C_{j|a_{\ell-1,j}; a_{1j} \dots a_{\ell-2,j}}(w_j^- | s_j^+)$,

22: **end if**

23: **end for**

24: **for** $j = \ell + 1, \dots, d$ **do**

25: **if** $a_{\ell,j} = m_{\ell,j}$ **then** $s_j^+ \leftarrow v_{m_{\ell+1,j}}^+$, $s_j^- \leftarrow v_{m_{\ell+1,j}}^-$,

26: **else if** $a_{\ell,j} < m_{\ell,j}$ **then** $s_j^+ \leftarrow v_{m_{\ell+1,j}}^+$, $s_j^- \leftarrow v_{m_{\ell+1,j}}^-$,

27: **end if**

28: $w_j^+ \leftarrow v_j^+$, $w_j^- \leftarrow v_j^-$,

29: **end for**

30: **end for**

31: Return v_d^+ .

study the asymptotic conditional CDF for a trivariate vine copula with bivariate Archimedean copulas and standard normal margins; the Archimedean assumption allows for some tractable results to be obtained. We give a classification of the conditional CDF based on the tail dependence properties of bivariate Archimedean copulas. Section 4.2.3 considers several special cases with different combinations of bivariate Archimedean copulas on the edges of a trivariate vine, and shows a number of different tail behaviors. Section 4.3 briefly discusses the possibility of generalize the results to higher dimensions.

4.1 Bivariate asymptotic conditional quantile

In this section, we focus on a bivariate random vector (X, Y) with standard normal margins. Let $C(u, v)$ be the copula, then the joint CDF is $F_{X,Y}(x, y) = C(\Phi(x), \Phi(y))$. Without loss of generality, we assume the copula $C(u, v)$ has positive dependence. We are interested in the shape of the conditional CDF $F_{Y|X}(y|x)$ and conditional quantile $F_{Y|X}^{-1}(\alpha|x)$, when x is extremely large or small and $\alpha \in (0, 1)$ is fixed. Bernard and Czado (2015) study a few special cases for bivariate copulas. Our results are more extensive in relating the shape of asymptotic quantiles to the strength of dependence in the joint tail.

If the conditional distribution $C_{V|U}(\cdot|u)$ converges to a continuous distribution with support on $[0, 1]$, as $u \rightarrow 0^+$, then $C_{V|U}^{-1}(\alpha|0) > 0$, for $\alpha \in (0, 1)$. Therefore, $F_{Y|X}^{-1}(\alpha|x)$ levels off as $x \rightarrow -\infty$. The same argument applies when $x \rightarrow +\infty$. That is,

$$\lim_{x \rightarrow -\infty} F_{Y|X}^{-1}(\alpha|x) = \Phi^{-1}(C_{V|U}^{-1}(\alpha|0)); \quad \lim_{x \rightarrow +\infty} F_{Y|X}^{-1}(\alpha|x) = \Phi^{-1}(C_{V|U}^{-1}(\alpha|1)).$$

If $C_{V|U}(\cdot|u)$ converges to a degenerate distribution at 0 when $u \rightarrow 0^+$, then $\lim_{u \rightarrow 0^+} C_{V|U}^{-1}(\alpha|u) = 0$. To study the shape of $F_{Y|X}(y|x)$ when x is very negative, we need to further investigate the rate at which $C_{V|U}^{-1}(\alpha|u)$ converges to 0. The next proposition, with proof in Appendix B, summarizes the possibilities.

Proposition 4.1. Let (X, Y) be a bivariate random vector with standard normal margins and a positively dependent copula $C(u, v)$.

- (Lower tail) Fixing $\alpha \in (0, 1)$, if $-\log C_{V|U}^{-1}(\alpha|u) \sim k_\alpha(-\log u)^\eta$ as $u \rightarrow 0^+$, then $F_{Y|X}^{-1}(\alpha|x) \sim -(2^{1-\eta}k_\alpha)^{1/2}|x|^\eta$ as $x \rightarrow -\infty$.
- (Upper tail) Fixing $\alpha \in (0, 1)$, if $-\log[1 - C_{V|U}^{-1}(\alpha|u)] \sim k_\alpha[-\log(1-u)]^\eta$ as $u \rightarrow 1^-$, then $F_{Y|X}^{-1}(\alpha|x) \sim (2^{1-\eta}k_\alpha)^{1/2}x^\eta$ as $x \rightarrow +\infty$.

Here η indicates the strength of relation between two variables in the tail; a larger η value corresponds to stronger relation. The strongest possible comonotonic dependence is when $Y = X$, and the conditional quantile function is $F_{Y|X}^{-1}(\alpha|x) = x$, which is linear in x and does not depend on α ; in this case, $\eta = 1$. The weakest possible positive dependence is when X and Y are independent, and $F_{Y|X}^{-1}(\alpha|x) = F_Y^{-1}(\alpha)$ does not depend on x ; in this case, $\eta = 0$. Based on the value of η , the asymptotic behavior of the conditional quantile function can be classified into the following categories:

1. Strong linear: $\eta = 1$ and $k_\alpha = 1$. $F_{Y|X}^{-1}(\alpha|x)$ goes to infinity linearly, and it does not depend on α . It has stronger dependence than bivariate normal.
2. Weak linear: $\eta = 1$, k_α can depend on α and $0 < k_\alpha < 1$. $F_{Y|X}^{-1}(\alpha|x)$ goes to infinity linearly and it depends on α . It has comparable dependence with bivariate normal.
3. Sublinear: $0 < \eta < 1$. $F_{Y|X}^{-1}(\alpha|x)$ goes to infinity sublinearly. The dependence is weaker than bivariate normal.
4. Asymptotic constant: $\eta = 0$. $F_{Y|X}^{-1}(\alpha|x)$ converges to a finite constant. Asymptotically it behaves like independent.

Figure 2 shows the conditional quantile functions for bivariate copulas with different η in the upper and lower tails. Example 4.1 to 4.2 derive the conditional quantile functions for bivariate Mardia-Takahasi-Clayton-Cook-Johnson (MTCJ) and Gumbel copulas. Note that η is constant over α for several commonly used

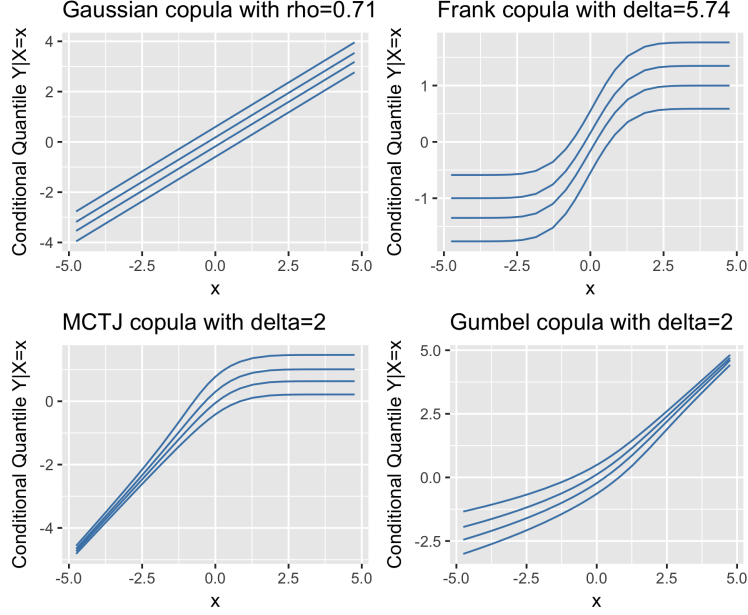


Figure 2: Conditional quantile functions for bivariate copulas with Kendall's $\tau = 0.5$. Quantile levels are 20%, 40%, 60% and 80%.

parametric bivariate copula families. However, there are cases where η depends on α . For example, the boundary conditional distribution of the bivariate Student- t copula has mass at both 0 and 1; depending on the value of α , $C_{V|U}^{-1}(\alpha|u)$ could go to either 0 or 1, as $u \rightarrow 0$.

Example 4.1. (MTCJ lower tail) The conditional quantile function of the bivariate MTCJ copula is

$$C_{V|U}^{-1}(\alpha|u; \delta) = [(\alpha^{-\delta/(1+\delta)} - 1)u^{-\delta} + 1]^{-1/\delta} \sim (\alpha^{-\delta/(1+\delta)} - 1)^{-1/\delta}u, \quad u \rightarrow 0; \quad \delta > 0.$$

Take the log of both sides, $-\log C_{V|U}^{-1}(\alpha|u; \delta) \sim \log u$. By Proposition 4.1, we have $F_{Y|X}^{-1}(\alpha|x) \sim x$, as $x \rightarrow -\infty$. To apply the next proposition to get the same conclusion, the generator is the gamma Laplace transform $\psi(s) = (1 + s)^{-1/\delta}$.

Example 4.2. (Gumbel lower tail) The conditional CDF of the bivariate Gumbel copula is

$$C_{V|U}(v|u; \delta) = u^{-1} \exp\{-[(-\log u)^\delta + (-\log v)^\delta]^{1/\delta}\} \left[1 + \left(\frac{-\log v}{-\log u}\right)^\delta\right]^{1/\delta-1}; \quad \delta > 1.$$

The conditional quantile function $C_{V|U}^{-1}(\alpha|u; \delta)$ does not have a closed-form expression; it has the following asymptotic expansion:

$$-\log C_{V|U}^{-1}(\alpha|u; \delta) \sim (-\delta \log \alpha)^{1/\delta} (-\log u)^{1-1/\delta}, \quad u \rightarrow 0.$$

By Proposition 4.1, we have $F_{Y|X}^{-1}(\alpha|x) \sim -(-2\delta \log \alpha)^{1/(2\delta)} |x|^{1-1/\delta}$, as $x \rightarrow -\infty$. To apply the next proposition to get the same conclusion, the generator is the positive stable Laplace transform $\psi(s) = \exp\{-s^{-1/\delta}\}$.

For Archimedean and survival Archimedean copulas, the following proposition provides a link between tail dependence behavior and tail conditional distribution and quantile functions. The proof of the proposition is included in Appendix C.

Proposition 4.2. Given the generator or Laplace transform (LT) ψ of an Archimedean copula, we assume the following.

1. For the upper tail of ψ , as $s \rightarrow +\infty$,

$$\psi(s) \sim T(s) = a_1 s^q \exp(-a_2 s^r) \quad \text{and} \quad \psi'(s) \sim T'(s), \quad (4.1)$$

where $a_1 > 0$, $r = 0$ implies $a_2 = 0$ and $q < 0$, and $r > 0$ implies $r \leq 1$ and q can be 0, negative or positive.

2. For the lower tail of ψ , as $s \rightarrow 0^+$, there is $M \in (k, k+1)$ such that

$$\psi(s) = \sum_{i=0}^k (-1)^i h_i s^i + (-1)^{k+1} h_{k+1} s^M + o(s^M), \quad s \rightarrow 0^+, \quad (4.2)$$

where $h_0 = 1$ and $0 < h_i < \infty$ for $i = 1, \dots, k+1$. If $0 < M < 1$, then $k = 0$.

Then we have the following.

- (Lower tail) If $v \in (0, 1)$ and $\alpha \in (0, 1)$ are fixed, then as $u \rightarrow 0$,

$$C_{V|U}(v|u) \sim \begin{cases} 1 + (q-1)\psi^{-1}(v) \left(\frac{u}{a_1}\right)^{-1/q} \rightarrow 1 & \text{if } r = 0, \\ 1 - a_2^{1/r} r \psi^{-1}(v) (-\log u)^{1-1/r} \rightarrow 1 & \text{if } 0 < r < 1, \\ \text{const} \in (0, 1) & \text{if } r = 1. \end{cases} \quad (4.3)$$

$$C_{V|U}^{-1}(\alpha|u) \sim \begin{cases} (\alpha^{1/(q-1)} - 1)^q \cdot u \rightarrow 0 & \text{if } r = 0, \\ \exp\left[-\left(\frac{-\log \alpha}{r}\right)^r (-\log u)^{1-r}\right] \rightarrow 0 & \text{if } 0 < r < 1, \\ \text{const} \in (0, 1) & \text{if } r = 1. \end{cases} \quad (4.4)$$

- (Upper tail) If $v \in (0, 1)$ and $\alpha \in (0, 1)$ are fixed, then as $u \rightarrow 1$,

$$C_{V|U}(v|u) \sim \begin{cases} -\frac{\psi'(\psi^{-1}(v))}{h_1^{1/M} M} (1-u)^{(1-M)/M} \rightarrow 0 & \text{if } 0 < M < 1, \\ \text{const} \in (0, 1) & \text{if } M > 1. \end{cases} \quad (4.5)$$

$$C_{V|U}^{-1}(\alpha|u) \sim \begin{cases} 1 - (\alpha^{1/(M-1)} - 1)^M (1-u) \rightarrow 1 & \text{if } 0 < M < 1, \\ \text{const} \in (0, 1) & \text{if } M > 1. \end{cases} \quad (4.6)$$

Note that we do not cover the case of $M = 1$ for the upper tail because it involves a slowly varying function. Combined with Proposition 4.1, it states that, for the lower tail, the three cases $r = 0$, $0 < r < 1$ and $r = 1$ correspond to strong linear, sublinear and asymptotic constant conditional quantile functions respectively; for the upper tail, the two cases $0 < M < 1$ and $M > 1$ correspond to strong linear and asymptotic constant conditional quantile functions respectively. Proposition 4.2 is used in Section 4.2.2 for analyzing cases of trivariate vine copulas.

4.2 Trivariate asymptotic conditional quantile

In this section, we aim to extend some results from the previous subsection to trivariate distributions. Specifically, we study the trivariate case $F_{Y|X_1, X_2}^{-1}(\alpha|x_1, x_2)$ with a trivariate vine copula model. However, extending from bivariate to trivariate is not trivial, since the asymptotic conditional quantile function depends on the direction in which (x_1, x_2) go to infinite.

4.2.1 Trivariate strongest functional relationship

We first study the strongest dependence: functional relationship between the response variable Y and explanatory variables X_1 and X_2 . Since the marginal distribution of Y does not have a closed-form expression in general, it is difficult to obtain a general result. We focus on a special case where the marginal distribution of Y can be calculated. It is shown that the conditional quantile function is asymptotically linear in x_1 or x_2 along a ray on the (x_1, x_2) -plane, and this is an extension of the bivariate strong linear case.

Let $Y^* = h(X_1^*, X_2^*)$, where h is monotonically increasing in each argument, $Y^* \sim F_{Y^*}$, $X_1^* \sim F_{X_1^*}$ and $X_2^* \sim F_{X_2^*}$. Transforming them to $N(0, 1)$ variables, we define $Y = \Phi^{-1}(F_{Y^*}(Y^*))$, $X_1 = \Phi^{-1}(F_{X_1^*}(X_1^*))$ and $X_2 = \Phi^{-1}(F_{X_2^*}(X_2^*))$. The following functional relationship holds

$$Y = \Phi^{-1} \circ F_{Y^*} \circ h \left(F_{X_1^*}^{-1}(\Phi(X_1)), F_{X_2^*}^{-1}(\Phi(X_2)) \right) := g(X_1, X_2). \quad (4.7)$$

We are interested in the conditional quantile $F_{Y|X_1, X_2}^{-1}(\alpha|x_1, x_2) = g(x_1, x_2)$. In this case, it is obvious that the conditional quantile function does not depend on the quantile level α . It is conjectured that it is a generalization of the bivariate strong linear case, in the sense that g is asymptotically linear as $(x_1, x_2) \rightarrow (\infty, \infty)$ or $(-\infty, -\infty)$ along different rays, even though g can be quite nonlinear in two variables.

We focus on a special case to gain insight into the asymptotic behavior of $g(x_1, x_2)$. Assume $Y^* = X_1^* + X_2^*$, and X_1^*, X_2^* follow $\text{Gamma}(\alpha_1, 1)$ and $\text{Gamma}(\alpha_2, 1)$ independently. As a result, Y^* follows $\text{Gamma}(\alpha_1 + \alpha_2, 1)$. Using tail expansions of the gamma CDF at 0 and ∞ , the following can be obtained:

- If $x_2 \sim kx_1$ as $x_1, x_2 \rightarrow +\infty$, then $g(x_1, x_2) \sim \sqrt{1 + k^2}x_1$.
- If $x_2 \sim kx_1$ as $x_1, x_2 \rightarrow -\infty$, then

$$g(x_1, x_2) \sim \begin{cases} \sqrt{\frac{\alpha_1 + \alpha_2}{\alpha_1}} x_1 & \text{if } k^2 \geq \frac{\alpha_2}{\alpha_1}, \\ \sqrt{\frac{\alpha_1 + \alpha_2}{\alpha_2}} kx_1 & \text{if } k^2 < \frac{\alpha_2}{\alpha_1}. \end{cases}$$

Detailed derivations can be found in Appendix D. Although the conditional quantile function is not linear in both x_1 and x_2 , it is asymptotically linear in x_1 or x_2 along a ray. Note that this is an asymptotic property and it is true only if x_1 and x_2 are large enough. The rate of asymptotic approximation depends on k, α_1 and α_2 because of the arguments $-x_1^2/(2\alpha_1)$ and $-k^2x_1^2/(2\alpha_2)$ in the exponential function.

4.2.2 Trivariate conditional boundary distribution with bivariate Archimedean copulas

For a trivariate vine copula model, it is difficult to get general results to cover all types of bivariate copulas for the vine, but it is possible to get results for the cases where all bivariate copulas are Archimedean. This provides some insight on the tail behavior of conditional quantile functions. Specifically, we study how the tail properties of the bivariate Archimedean copulas on the edges affect the asymptotic behavior of the conditional CDF. It turns out that trivariate cases are more complex than bivariate ones. For a bivariate Archimedean copula, the boundary conditional CDF $C_{V|U}(v|0)$ is either a distribution with support on all of $(0, 1)$ or a degenerate distribution at 0. However, depending on the bivariate copulas on the edges, the conditional CDF $C_{3|12}(v|u_1, u_2)$ could be a distribution with support on all of $(0, 1)$, a degenerate distribution at 0, or a degenerate distribution at 1 (the unusual case), as $(u_1, u_2) \rightarrow (0, 0)$ along a ray. The results are summarized in Tables 1 and 2.

Some results on the asymptotic conditional distributions of bivariate Archimedean copulas are presented in Appendix C. Based on those results, we study the conditional distribution of trivariate vine copulas with bivariate Archimedean copulas. Specifically, we are interested in the boundary conditional distribution of a trivariate vine copula with C_{12}, C_{23} in tree 1 and $C_{13;2}$ in tree 2:

$$u_{3|12} := C_{3|12}(v|u_1, u_2) = C_{3|1;2}(u_{3|2}|u_{1|2}), \quad (4.8)$$

where $u_{3|2} := C_{3|2}(v|u_2)$ and $u_{1|2} := C_{1|2}(u_1|u_2)$, $C_{3|1;2}(b|a) = \partial C_{13;2}(a, b)/\partial a$, $v \in (0, 1)$ and $(u_1, u_2) \rightarrow (0, 0)$ or $(u_1, u_2) \rightarrow (1, 1)$. $C_{1|2}, C_{3|2}$ and $C_{3|1;2}$ are the conditional copulas of C_{12}, C_{23} and $C_{13;2}$ respectively.

		$\lim_{u_2 \rightarrow 0} C_{3 2}(v u_2)$					
		(0, 1)			1		
$\lim_{u_1, u_2 \rightarrow 0} C_{1 2}(u_1 u_2)$	0	(0, 1)	1	1	1	1	1
	(0, 1)	(0, 1)	(0, 1)	(0, 1)	1	1	1
	1	(0, 1)	(0, 1)	0	1	1	*
$C_{13;2}$		$\kappa_{13} = 2$	$\kappa_{13} \in (1, 2)$	$\kappa_{13} = 1$	$\kappa_{13} = 2$	$\kappa_{13} \in (1, 2)$	$\kappa_{13} = 1$

Table 1: The taxonomy of the lower tail boundary conditional distribution $\lim_{u_1, u_2 \rightarrow 0} u_{3|12}$, where $u_{3|12}$ is defined in (4.8). The first and third rows correspond to κ_{13L} and κ_{13U} respectively.

As $(u_1, u_2) \rightarrow (0, 0)$, $u_{3|12}$ can, in some cases, depend on $C_{3|1;2}(\cdot|0)$ or $C_{3|1;2}(\cdot|1)$, as well as $C_{3|2}(\cdot|0)$ and $C_{1|2}(\cdot|0)$. Similarly, as $(u_1, u_2) \rightarrow (1, 1)$, $u_{3|12}$ can, in some cases, depend on $C_{3|1;2}(\cdot|0)$ or $C_{3|1;2}(\cdot|1)$, as well as $C_{3|2}(\cdot|1)$ and $C_{1|2}(\cdot|1)$. This is why the trivariate and higher-dimensional cases of boundary conditional CDF can be complicated. Also, in some cases, the form of the boundary conditional CDF depends on the direction of $(u_1, u_2) \rightarrow (0, 0)$ or $(1, 1)$.

Given the copula boundary conditional distribution $u_{3|12}$, we can obtain its equivalence on the normal scale. Let the trivariate vine copula be the CDF of a random vector (U_1, U_2, V) , and define $X_1 = \Phi^{-1}(U_1)$, $X_2 = \Phi^{-1}(U_2)$ and $Y = \Phi^{-1}(V)$. We are interested in the conditional quantile function $F_{Y|X_1, X_2}^{-1}(\alpha|x_1, x_2)$, as $x_1, x_2 \rightarrow -\infty$ and x_1/x_2 converges to a constant. For a fixed quantile level α ,

- If $u_{3|12} \rightarrow 0$ as $(u_1, u_2) \rightarrow (0, 0)$ and $u_2 \sim u_1^k$, then $F_{Y|X_1, X_2}^{-1}(\alpha|x_1, x_2) \rightarrow +\infty$ as $x_1, x_2 \rightarrow -\infty$ and $x_2/x_1 \rightarrow \sqrt{k}$;
- If $u_{3|12}$ converges to a constant in $(0, 1)$ as $(u_1, u_2) \rightarrow (0, 0)$ and $u_2 \sim u_1^k$, then $F_{Y|X_1, X_2}^{-1}(\alpha|x_1, x_2)$ converges to a finite constant as $x_1, x_2 \rightarrow -\infty$ and $x_2/x_1 \rightarrow \sqrt{k}$;
- If $u_{3|12} \rightarrow 1$ as $(u_1, u_2) \rightarrow (0, 0)$ and $u_2 \sim u_1^k$, then $F_{Y|X_1, X_2}^{-1}(\alpha|x_1, x_2) \rightarrow -\infty$ as $x_1, x_2 \rightarrow -\infty$ and $x_2/x_1 \rightarrow \sqrt{k}$.

Similar results hold for the upper tail, that is $u_1, u_2 \rightarrow 1$ and $u_2 \sim u_1^k$.

Trivariate vine copula lower tail

Fix $v \in (0, 1)$ and let $u_1, u_2 \rightarrow 0$ with $u_2 \sim u_1^k$. According to (C.2) and (C.6), depending on the tail order of $C_{23}(u_2, u_3)$, the limit of $u_{3|2} = C_{3|2}(v|u_2)$ could either be a number in $(0, 1)$, or 1. Similarly, according to Appendix C.1, the limit of $u_{1|2} = C_{1|2}(u_1|u_2)$ could either be 0, a number in $(0, 1)$, or 1. Depending on the limit of $u_{1|2}$, we also need to take the corresponding tail behavior of $C_{13;2}$ into consideration. The possible combinations of the tail behaviors are summarized in Table 1.

The first row of Table 1 corresponds to $u_{1|2} \rightarrow 0$.

- If $\lim_{u_2 \rightarrow 0} u_{3|2} \in (0, 1)$ and $C_{13;2}$ has $\kappa_{13L} = 2$, then $\text{support}(C_{3|1;2}(\cdot|0)) = (0, 1)$. Therefore $\lim_{u_1, u_2 \rightarrow 0} u_{3|12} \in (0, 1)$, as shown in row 1, column 1.
- If $\lim_{u_2 \rightarrow 0} u_{3|2} \in (0, 1)$ and $C_{13;2}$ has $\kappa_{13L} \in [1, 2)$, then $C_{3|1;2}(\cdot|0)$ is a degenerate distribution with a point mass at 0. Therefore $u_{3|12} \rightarrow 1$, as shown in row 1, columns 2–3.
- If $u_{3|2} \rightarrow 1$, then $u_{3|12} \rightarrow 1$, regardless of the tail behavior of $C_{13;2}$. This is shown in row 1, columns 4–6.

The second row of Table 1 corresponds to $\lim_{u_1, u_2 \rightarrow 0} u_{1|2} \in (0, 1)$. In this case, the tail behavior of $C_{13;2}$ is irrelevant. If $\lim_{u_2 \rightarrow 0} u_{3|2} \in (0, 1)$, then $\lim_{u_1, u_2 \rightarrow 0} u_{3|12} \in (0, 1)$ (row 2, columns 1–3); if $\lim_{u_2 \rightarrow 0} u_{3|2} = 1$, then $\lim_{u_1, u_2 \rightarrow 0} u_{3|12} = 1$ (row 2, columns 4–6).

The third row of Table 1 corresponds to $u_{1|2} \rightarrow 1$.

- If $\lim_{u_2 \rightarrow 0} u_{3|2} \in (0, 1)$ and $C_{13;2}$ has $\kappa_{13U} \in (1, 2]$, then $\text{support}(C_{3|1;2}(\cdot|1)) = (0, 1)$. Therefore $\lim_{u_1, u_2 \rightarrow 0} u_{3|12} \in (0, 1)$, as shown in row 3, columns 1–2.

		$\lim_{u_2 \rightarrow 0} C_{3 2}(v u_2)$					
		0			(0, 1)		
$\lim_{u_1, u_2 \rightarrow 0} C_{1 2}(u_1 u_2)$	0	0	0*	†	(0, 1)	1	1
	(0, 1)	0	0	0	(0, 1)	(0, 1)	(0, 1)
	1	0	0	0	(0, 1)	(0, 1)	0
$C_{13;2}$		$\kappa_{13} = 2$	$\kappa_{13} \in (1, 2)$	$\kappa_{13} = 1$	$\kappa_{13} = 2$	$\kappa_{13} \in (1, 2)$	$\kappa_{13} = 1$

Table 2: The taxonomy of the upper tail boundary conditional distribution $\lim_{u_1, u_2 \rightarrow 1} u_{3|12}$, where $u_{3|12}$ is defined in (4.8). The first and third rows correspond to κ_{13L} and κ_{13U} respectively.

- If $\lim_{u_2 \rightarrow 0} u_{3|2} \in (0, 1)$ and $C_{13;2}$ has $\kappa_{13U} = 1$, then $C_{3|1;2}(\cdot|1)$ is a degenerate distribution with a point mass at 1. Therefore $u_{3|12} \rightarrow 0$, as shown in row 3, column 3.
- If $u_{3|2} \rightarrow 1$ and $C_{13;2}$ has $\kappa_{13U} \in (1, 2]$, then $\text{support}(C_{3|1;2}(\cdot|1)) = (0, 1)$. Therefore $u_{3|12} \rightarrow 1$, as shown in row 3, columns 4–5.
- If $u_{3|2} \rightarrow 1$ and $C_{13;2}$ has $\kappa_{13U} = 1$, then $C_{3|1;2}(\cdot|1)$ is a degenerate distribution with a point mass at 1. The limit of $u_{3|12}$ is unclear and needs further investigation (row 3, column 6, cell *). Depending on κ_{23L} , we have the following results. (See Appendix E for a detailed derivation.)
 - If C_{23} has $\kappa_{23L} \in (1, 2)$, then $C_{3|1;2}(u_{3|2}|u_{1|2}) \rightarrow 0$.
 - If C_{23} has $\kappa_{23L} = 1$, then

$$C_{3|1;2}(u_{3|2}|u_{1|2}) \rightarrow \begin{cases} 1 & \text{if } -q_{23}^{-1} - q_{12}^{-1}(k^- - 1) > 0, \\ \text{const} \in (0, 1) & \text{if } -q_{23}^{-1} - q_{12}^{-1}(k^- - 1) = 0, \\ 0 & \text{if } -q_{23}^{-1} - q_{12}^{-1}(k^- - 1) < 0, \end{cases}$$

where q_{23} and q_{12} are the parameters of ψ_{23} for C_{23} and ψ_{12} for C_{12} respectively.

Trivariate vine copula upper tail

Fix $v \in (0, 1)$ and let $(u_1, u_2) \rightarrow (1, 1)$ with $(1 - u_2) \sim (1 - u_1)^k$. According to (C.10), depending on the tail order of $C_{23}(u_2, u_3)$, the limit of $u_{3|2} = C_{3|2}(v|u_2)$ could either be a number in $(0, 1)$, or 0. Similarly, according to Appendix C.2, the limit of $u_{1|2} = C_{1|2}(u_1|u_2)$ could either be 0, a number in $(0, 1)$, or 1. Depending on the limit of $u_{1|2}$, we also need to take the corresponding tail behavior of $C_{13;2}$ into consideration. The possible combinations of the tail behaviors are summarized in Table 2.

The first row of Table 2 corresponds to $u_{1|2} \rightarrow 0$.

- If $u_{3|2} \rightarrow 0$ and $C_{13;2}$ has $\kappa_{13L} = 2$, then $\text{support}(C_{3|1;2}(\cdot|0)) = (0, 1)$. Therefore $u_{3|12} \rightarrow 0$, as shown in row 1, column 1.
- If $u_{3|2} \rightarrow 0$ and $C_{13;2}$ has $\kappa_{13L} \in (1, 2)$, then $C_{3|1;2}(\cdot|0)$ is a degenerate distribution with a point mass at 0. The limit of $u_{3|12}$ is unclear and needs further investigation (row 1, column 2, cell *). It can be shown that in that case, $u_{1|2} \rightarrow 0$. See Appendix E for a detailed derivation.
- If $u_{3|2} \rightarrow 0$ and $C_{13;2}$ has $\kappa_{13L} = 1$, then $C_{3|1;2}(\cdot|0)$ is a degenerate distribution with a point mass at 0. The limit of $u_{3|12}$ is unclear and needs further investigation (row 1, column 3, cell †). Depending on the relationship among M_{12} , M_{23} and k , we have the following results. (See Appendix E for a detailed derivation.)

$$C_{3|1;2}(u_{3|2}|u_{1|2}) \rightarrow \begin{cases} 0 & \text{if } -\frac{M_{23}-1}{M_{23}} - \frac{M_{12}-1}{M_{12}}\left(\frac{1}{k} - 1\right) > 0, \\ \text{const} \in (0, 1) & \text{if } -\frac{M_{23}-1}{M_{23}} - \frac{M_{12}-1}{M_{12}}\left(\frac{1}{k} - 1\right) = 0, \\ 1 & \text{if } -\frac{M_{23}-1}{M_{23}} - \frac{M_{12}-1}{M_{12}}\left(\frac{1}{k} - 1\right) < 0, \end{cases}$$

where M_{23} and M_{12} are the parameters of ψ_{23} for C_{23} and ψ_{12} for C_{12} respectively.

- If $\lim_{u_2 \rightarrow 1} u_{3|2} \in (0, 1)$ and $C_{13;2}$ has $\kappa_{13L} = 2$, then $\text{support}(C_{3|1;2}(\cdot|0)) = (0, 1)$. Therefore $\lim_{(u_1, u_2) \rightarrow (0,0)} u_{3|12} \in (0, 1)$, as shown in row 1, column 4.
- If $\lim_{u_2 \rightarrow 1} u_{3|2} \in (0, 1)$ and $C_{13;2}$ has $\kappa_{13L} \in [1, 2)$, then $C_{3|1;2}(\cdot|0)$ is a degenerate distribution with a point mass at 0. Therefore $u_{3|12} \rightarrow 1$, as shown in row 1, columns 5–6.

The second row of Table 2 corresponds to $\lim_{u_1, u_2 \rightarrow (1,1)} u_{1|2} \in (0, 1)$. In this case, the tail behavior of $C_{13;2}$ is irrelevant. If $\lim_{u_2 \rightarrow 1} u_{3|2} = 0$, then $\lim_{u_1, u_2 \rightarrow (1,1)} u_{3|12} = 0$ (row 2, columns 1–3); if $\lim_{u_2 \rightarrow 1} u_{3|2} \in (0, 1)$, then $\lim_{u_1, u_2 \rightarrow (1,1)} u_{3|12} \in (0, 1)$ (row 2, columns 4–6).

The third row of Table 2 corresponds to $u_{1|2} \rightarrow 1$.

- If $u_{3|2} \rightarrow 0$, then $u_{3|12} \rightarrow 0$, regardless of the tail property of $C_{13;2}$. This is shown in row 3, columns 1–3.
- If $\lim_{u_2 \rightarrow 1} u_{3|2} \in (0, 1)$ and $C_{13;2}$ has $\kappa_{13U} = 2$, then $\text{support}(C_{3|1;2}(\cdot|1)) = (0, 1)$. Therefore $\lim_{u_1, u_2 \rightarrow 0} u_{3|12} \in (0, 1)$, as shown in row 3, columns 4–5.
- If $\lim_{u_2 \rightarrow 1} u_{3|2} \in (0, 1)$ and $C_{13;2}$ has $\kappa_{13U} = 2$, then $C_{3|1;2}(\cdot|1)$ is a degenerate distribution with a point mass at 1. Therefore $u_{3|12} \rightarrow 0$, as shown in row 3, column 6.

4.2.3 Case studies: trivariate conditional quantile

In this section, we provide a few examples to illustrate how to use the results in Table 1 and Table 2 to derive the boundary conditional quantiles for trivariate vine with bivariate Archimedean copulas. Analytic results are provided for those examples to illustrate how the tail properties of bivariate copulas on edges of the vine can affect asymptotic properties of conditional quantiles. We use the same setting as before: $v \in (0, 1)$ and $u_1, u_2 \rightarrow (0, 0)$ or $u_1, u_2 \rightarrow (1, 1)$; we are interested in the limit of $u_{3|12} = C_{3|1;2}(u_{3|1}|u_{1|2})$ as well as the conditional quantile function on the normal scale.

In case 1, the two linking copulas to Y have $\kappa_U = 1$ and $\kappa_L \in (1, 2)$. In case 2, the linking copulas to Y have $\kappa_U = \kappa_L = 2$. The less straightforward case 3 has $\kappa_U = \kappa_L = 2$ for the linking copula to Y in tree 1 and $\kappa_U = 1, \kappa_L \in (1, 2)$ for the linking copula to Y in tree 2.

Case 1

C_{12} , C_{23} and $C_{13;2}$ are all bivariate Gumbel copulas, with lower tail intermediate dependence and upper tail dependence.

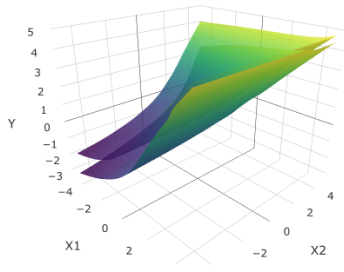
Lower tail ($u_1, u_2 \rightarrow (0, 0)$): C_{12} has $\kappa_{12L} \in (1, 2)$. According to (C.8), $u_{1|2} \rightarrow 0$. C_{23} has $\kappa_{23L} \in (1, 2)$. According to (C.6), $u_{3|2} \rightarrow 1$. Finally, $C_{13;2}$ has $\kappa_{13L} \in (1, 2)$. The combination of the three copulas corresponds to the row 1 column 5 in Table 1, that is $u_{3|12} \rightarrow 1$. On the normal scale, the conditional quantile $F_{Y|X_1, X_2}^{-1}(\alpha|x_1, x_2) \rightarrow -\infty$ as $x_1, x_2 \rightarrow -\infty$. A more detailed analysis (see Appendix F) shows that

$$F_{Y|X_1, X_2}^{-1}(\alpha|x_1, x_2) = O\left(\left(-\log \alpha\right)^{r_{23}r_{13;2}/2}|x_2|^{1-r_{23}r_{13;2}}\right), \quad x_1, x_2 \rightarrow -\infty, x_2/x_1 \rightarrow \sqrt{k},$$

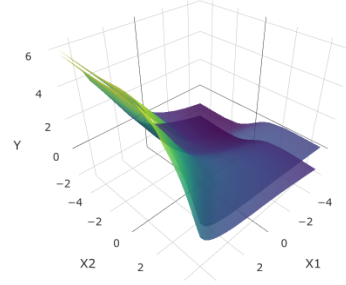
where r_{23} and $r_{13;2}$ are parameters of the LT ψ_{23} for C_{23} and $\psi_{13;2}$ for $C_{13;2}$ respectively. Since $1 - r_{23}r_{13;2} < 1$, the conditional quantile function goes to $-\infty$ sublinearly with respect to x_1 or x_2 .

Upper tail ($u_1, u_2 \rightarrow (1, 1)$): C_{23} has $\kappa_{23U} = 1$. According to (C.10), $u_{3|2} \rightarrow 0$. C_{12} has $\kappa_{12U} = 1$. Applying (C.13), we need to investigate the rate at which u_1 and u_2 go to 1. Assuming $(1 - u_2) \sim (1 - u_1)^k$:

- If $k > 1$, then $u_{1|2} \rightarrow 0$. $C_{13;2}$ has $\kappa_{13L} \in (1, 2)$. This corresponds to row 1 column 2 in Table 2, that is $u_{3|12} \rightarrow 0$.
- If $k = 1$, then $\lim u_{1|2} \in (0, 1)$. This corresponds to row 2 columns 1–3 in Table 2, that is $\lim u_{3|12} \rightarrow 0$.
- If $0 < k < 1$, then $u_{1|2} \rightarrow 1$. We need to focus on the upper tail of $C_{13;2}$, which has $\kappa_{32U} = 1$. This corresponds to row 3 column 3 in Table 2, that is $u_{3|12} \rightarrow 0$.



(a) Case 1: as $x_1, x_2 \rightarrow +\infty$, the conditional quantile goes to $+\infty$ linearly; as $x_1, x_2 \rightarrow -\infty$, the conditional quantile goes to $-\infty$ sublinearly.



(b) Case 3: as $x_1, x_2 \rightarrow +\infty$ at different rates, the conditional quantile could either go up or down.

Figure 3: Conditional quantile surface $F_{Y|X_1, X_2}^{-1}(\alpha|x_1, x_2)$ in cases 1 and 3, for $\alpha = 0.25$ and 0.75 .

Therefore, $u_{3|12} \rightarrow 0$ regardless of the value of k . On the normal scale, the conditional quantile $F_{Y|X_1, X_2}^{-1}(\alpha|x_1, x_2) \rightarrow +\infty$ as $x_1, x_2 \rightarrow +\infty$. A more detailed analysis shows that, if $x_2/x_1 \rightarrow \sqrt{k}$ as $x_1, x_2 \rightarrow +\infty$, then

$$F_{Y|X_1, X_2}^{-1}(\alpha|x_1, x_2) \sim \begin{cases} x_2 & \text{if } k \geq 1, \\ \sqrt{1 + \frac{M_{23}}{M_{12}} \left(\frac{1}{k} - 1\right) x_2} & \text{if } 0 < k < 1. \end{cases}$$

In summary, as x_1 and x_2 go to $+\infty$, the conditional quantile goes to $+\infty$ linearly; as x_1 and x_2 go to $-\infty$, the conditional quantile goes to $-\infty$ sublinearly. This is a natural extension of the conditional quantile function of the bivariate Gumbel copula. Figure 3a shows the conditional quantile $F_{Y|X_1, X_2}^{-1}(\alpha|x_1, x_2)$ for $\alpha = 0.25$ and 0.75 . The parameters of the copulas δ_{12} , δ_{23} , and $\delta_{13;2}$ are chosen such that the corresponding Spearman correlation $\rho_S = 0.5$.

Case 2

- C_{12} is a bivariate Frank copula, with $\kappa_{12L} = \kappa_{12U} = 2$.
- C_{23} is a bivariate Frank copula, with $\kappa_{23L} = \kappa_{23U} = 2$.
- $C_{13;2}$ could be any bivariate copula.

In this case, row 2 columns 1–3 in Table 1 and row 2 column 4–6 in Table 2 apply. That is, $\lim_{u_1, u_2 \rightarrow (0,0)} u_{3|12} \in (0, 1)$ and $\lim_{u_1, u_2 \rightarrow (1,1)} u_{3|12} \in (0, 1)$. On the normal scale, the conditional quantile $F_{Y|X_1, X_2}^{-1}(\alpha|x_1, x_2)$ converges to a finite constant as $x_1, x_2 \rightarrow +\infty$ or $-\infty$. This example shows that, if the bivariate copulas on the first level has $\kappa_L = 2$ (or $\kappa_U = 2$), then regardless of the second level copula, the conditional lower (upper) quantile is asymptotically constant.

Case 3

- C_{12} is a bivariate Gumbel copula, with $\kappa_{12L} \in (1, 2)$ and $\kappa_{12U} = 1$.
- C_{23} is a bivariate Frank copula, with $\kappa_{23L} = \kappa_{23U} = 2$.
- $C_{13;2}$ is a bivariate Gumbel copula, with $\kappa_{13L} \in (1, 2)$ and $\kappa_{13U} = 1$.

Lower tail ($u_1, u_2 \rightarrow (0, 0)$): C_{12} has $\kappa_{12L} \in (1, 2)$. According to (C.8), $u_{1|2} \rightarrow 0$ and $-\log u_{1|2} \sim O(-\log u_2)$. Since C_{23} has $\kappa_{23L} = 2$ and $\text{support}(C_{3|2}(\cdot|0)) = (0, 1)$, $\lim_{u_2 \rightarrow 0} u_{3|2} \in (0, 1)$. Finally, $C_{13;2}$

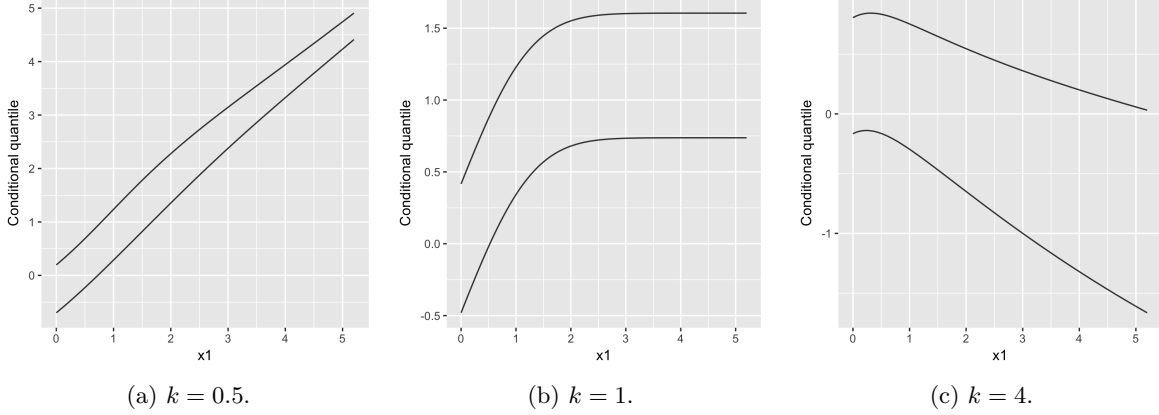


Figure 4: Conditional quantile $F_{Y|X_1, X_2}^{-1}(\alpha|x_1, x_2)$ versus x_1 in case 3 for $\alpha = 0.25$ and 0.75 , as $x_1 \rightarrow +\infty$. It shows that the conditional quantile converges to $+\infty$, a finite number, or $-\infty$.

has $\kappa_{13L} \in (1, 2)$. The combination of the three copulas corresponds to the row 1 column 2 in Table 1, that is $u_{3|12} \rightarrow 1$. On the normal scale, the conditional quantile $F_{Y|X_1, X_2}^{-1}(\alpha|x_1, x_2) \rightarrow -\infty$ as $x_1, x_2 \rightarrow -\infty$. According to Proposition 4.2, the conditional quantile $F_{Y|X_1, X_2}^{-1}(\alpha|x_1, x_2)$ is sublinear with respect to x_1 or x_2 , if $x_2/x_1 \rightarrow \sqrt{k}$.

Upper tail ($u_1, u_2 \rightarrow (1, 1)$): Since C_{23} has $\kappa_{23U} = 2$ and $\text{support}(C_{3|2}(\cdot|1)) = (0, 1)$, $\lim_{u_2 \rightarrow 1} u_{3|2} \in (0, 1)$. C_{12} has $\kappa_{12U} = 1$. Applying (C.13), we need to investigate the rate at which u_1 and u_2 go to 1. Assuming $(1 - u_2) \sim (1 - u_1)^k$:

- If $k > 1$, then $u_{1|2} \rightarrow 0$. $C_{13;2}$ has $\kappa_{13L} \in (1, 2)$. This corresponds to row 1 column 5 in Table 2, that is $u_{3|12} \rightarrow 1$. On the normal scale, the conditional quantile $F_{Y|X_1, X_2}^{-1}(\alpha|x_1, x_2) \rightarrow -\infty$ as $x_1, x_2 \rightarrow +\infty$ and $x_2/x_1 \rightarrow \sqrt{k}$. The conditional quantile $F_{Y|X_1, X_2}^{-1}(\alpha|x_1, x_2)$ is sublinear with respect to x_1 or x_2 .
- If $k = 1$, then $\lim u_{1|2} \in (0, 1)$. This corresponds to row 2 columns 4–6 in Table 2, that is $\lim u_{3|12} \in (0, 1)$. On the normal scale, the conditional quantile $F_{Y|X_1, X_2}^{-1}(\alpha|x_1, x_2)$ converges to a finite number as $x_1, x_2 \rightarrow +\infty$ and $x_2/x_1 \rightarrow 1$.
- If $0 < k < 1$, then $u_{1|2} \rightarrow 1$. We need to focus on the upper tail of $C_{13;2}$, which has $\kappa_{13U} = 1$. This corresponds to row 3 column 6 in Table 2, that is $u_{3|12} \rightarrow 0$. On the normal scale, the conditional quantile $F_{Y|X_1, X_2}^{-1}(\alpha|x_1, x_2) \rightarrow +\infty$ as $x_1, x_2 \rightarrow +\infty$ and $x_2/x_1 \rightarrow \sqrt{k}$. The conditional quantile $F_{Y|X_1, X_2}^{-1}(\alpha|x_1, x_2)$ is linear with respect to x_1 or x_2 .

Figure 3b shows the conditional quantile surface for $\alpha = 0.25$ and 0.75 . The parameters of the copulas δ_{12} , δ_{23} , and $\delta_{13;2}$ are chosen such that the corresponding Spearman correlation $\rho_S = 0.5$. Depending on the rate at which x_1 and x_2 go to $+\infty$, the conditional quantile could go to $+\infty$ or $-\infty$. Figure 4 shows the conditional quantile $F_{Y|X_1, X_2}^{-1}(\alpha|x_1, x_2)$ for $\alpha = 0.25$ and 0.75 as $x_1, x_2 \rightarrow \infty$ and $x_2/x_1 \rightarrow \sqrt{k}$, for $k = 0.5, 1$ and 4 . The three cases correspond to weak linear, asymptotic constant, and sublinear. This example also shows that the asymptotic behavior of the conditional quantile function varies depending on the direction along which x_1 and x_2 take.

The case of $k > 1$ and $F_{Y|X_1, X_2}^{-1}(\alpha|x_1, x_2) \rightarrow -\infty$ as $x_1, x_2 \rightarrow +\infty$ is unusual, given that all three copulas have positive dependence. One possible explanation is that, variable X_1 has strong tail dependence link to Y , and variable X_2 has tail quadrant independence link to Y ; when $k > 1$, X_2 goes to infinity faster than X_1 and the direction to limit is more concentrated on the weaker variable.

4.3 Beyond trivariate

Using the results in Appendix C and Section 4.2.2 as building blocks, the boundary conditional distribution of a higher-dimensional vine copula can be derived. Take a 4-dimensional vine copula as an example: without

loss of generality, we consider a D-vine copula with 1-2-3-4 as the first level tree. The conditional CDF can be represented by

$$u_{4|123} := C_{4|123}(v|u_1, u_2, u_3) = C_{4|1;23}(u_{4|23}|u_{1|23}),$$

where $u_{4|23} := C_{4|2;3}(u_{4|3}|u_{2|3})$, $u_{1|23} := C_{1|3;2}(u_{1|2}|u_{3|2})$, $u_{1|2} := C_{1|2}(u_1|u_2)$, $u_{2|3} = C_{2|3}(u_2|u_3)$, $u_{3|2} = C_{3|2}(u_3|u_2)$, $u_{4|3} = C_{4|3}(v|u_3)$, and $v \in (0, 1)$, $u_1, u_2, u_3 \rightarrow 0$ or 1 . Applying the techniques demonstrated in Section 4.2.2, the asymptotic behavior of $u_{4|23}$ and $u_{1|23}$ can be obtained. Afterwards, the results in Appendix C can be applied to get the limit of $u_{4|123}$. The limit of $u_{4|123}$ could be summarized as a table like Table 1 and Table 2, but it would be complicated to classify all the possible combinations of the bivariate copula tail behavior. Technically, the idea could be further generalized to any high dimensions.

A general heuristic statement is that if the more linking copulas of the X 's to Y have $\kappa = 1$, then the tail behavior of conditional quantiles is more likely to be asymptotically linear or sublinear. If all of the linking copulas of the X 's to Y have $\kappa = 2$, then the tail behavior of conditional quantiles is asymptotically constant.

5 Simulation study

We demonstrate the flexibility and effectiveness of vine copula regression methods by visualizing the fitted models on a simulated dataset. The simulated dataset has three variables: X_1 and X_2 are the explanatory variables and Y is the response variable; X_1 and X_2 are independent $N(0, 1)$ random variables, and Y is simulated in three settings with varying conditional expectations and variance structures. Let $U_1 = \Phi(X_1)$ and $U_2 = \Phi(X_2)$, where Φ is the standard normal CDF. ϵ is a random error following a standard normal distribution and independent from X_1 and X_2 . The three settings are as follows:

1. Linear and homoscedastic: $Y = 10X_1 + 5X_2 + 10\epsilon$.
2. Linear and heteroscedastic: $Y = 10X_1 + 5X_2 + 10(U_1 + U_2)\epsilon$.
3. Non-linear and heteroscedastic: $Y = U_1e^{1.8U_2} + 0.5(U_1 + U_2)\epsilon$.

We simulate 2000 samples for each setting and the samples are equally split to a training set and a test set. Four methods are considered in the simulation study: linear regression, quadratic regression, Gaussian copula, and vine copula. The Gaussian copula can be considered as a special case of the vine copula, in which the bivariate copula families on the vine edges are all bivariate Gaussian. Models are trained on the training set and used to obtain the conditional expectations as point predictions and 95% prediction intervals on the test set. For the Gaussian and vine copula, the marginal distribution of Y is modeled by a normal distribution in setting 1, and skew-normal distributions in settings 2 and 3.

To evaluate the performance of a regression model, we use root-mean-square error and out-of-sample log-likelihood.

- Root-mean-square error (RMSE) measures a model's performance on point estimation.

$$RMSE(\mathcal{M}) = \sqrt{\frac{1}{n_{\text{test}}} \sum_{i=1}^{n_{\text{test}}} (y_i - \hat{y}_i^{\mathcal{M}})^2},$$

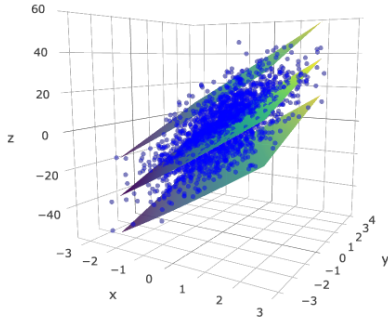
where y_i is the response variable of the i -th sample in the test set, and $\hat{y}_i^{\mathcal{M}}$ is the predicted conditional expectation of a fitted model \mathcal{M} .

- Out-of-sample log-likelihood (OOSLLK) is a score that can be used to compare models. It is closely related to the generalization error in machine learning literature (Chapter 7.2 in Hastie et al. (2009)).

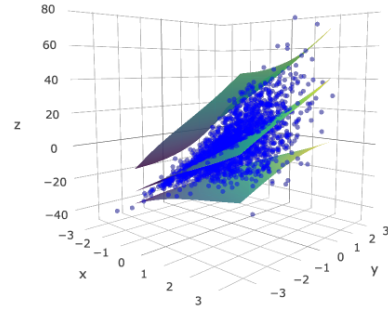
$$OOSLLK(\mathcal{M}) = \frac{1}{n_{\text{test}}} \sum_{i=1}^{n_{\text{test}}} \log \hat{f}_{Y|X_1, X_2}^{\mathcal{M}}(y_i | x_{i1}, x_{i2}),$$

where (x_{i1}, x_{i2}, y_i) is the i th observation in the test set, and $\hat{f}_{Y|X_1, X_2}^{\mathcal{M}}$ is the predicted conditional PDF of model \mathcal{M} . For example, if \mathcal{M} is a linear regression, then the predicted conditional distribution is

Linear and homoscedastic - Vine copula regression



Linear and heteroscedastic - Vine copula regression



(a) Linear and homoscedastic - Vine copula regression. (b) Linear and heteroscedastic - Vine copula regression.

Figure 5: Linear homoscedastic and linear heteroscedastic simulation settings.

a scaled and shifted t -distribution. If \mathcal{M} is a vine copula, the predicted conditional distribution can be calculated using the procedure described in Section 3.2. Note that the RMSE is not meaningful if there is heteroscedasticity in conditional distributions. OOSLLK adjusts for the non-constant variance if the true model is multivariate Gaussian.

The first setting serves as a sanity check; if the response variable is linear in the explanatory variables and the conditional variance is constant, the vine copula should behave like linear regression. Figure 5a plots the simulated data, the conditional expectation surface and 95% prediction interval surfaces. All three surfaces truthfully reflect the linearity of the data. The first two lines of Table 3 show that the vine copula and linear regression have the same RMSE and OOSLLK.

The second setting adds heteroscedasticity to the first setting; that is, the variance of Y increases as X_1 or X_2 increases while the linear relationship remains the same. We expect the conditional expectation surface to be linear. Figure 5b shows the prediction results of the vine copula. The conditional expectation surface is linear and the lengths of prediction intervals increase with X_1 and X_2 . The performance measures in Table 3 are also consistent with our expectation: the RMSEs are similar and the vine copula has higher OOSLLK.

Finally, the third setting incorporates both non-linearity and heteroscedasticity. Since the linear regression obviously cannot fit the non-linear trend, we compare our model to quadratic regression as well. Figure 6 shows the predicted surfaces for the three models. Although the quadratic regression model captures the non-linear trend, it is not flexible enough to model heteroscedasticity. Another drawback of quadratic regression is that, the conditional mean \hat{y} is not always monotonically increasing with respect to x_1 and x_2 , and this contradicts the pattern in the data. The vine copula naturally fits the non-linearity and heteroscedasticity pattern. Quantitatively, the vine copula outperforms the other two regressions based on both RMSE and OOSLLK, as shown in Table 3.

6 Application

6.1 Abalone data set

In this section, we apply the vine copula regression method on a real data set: the Abalone data set (Lichman, 2013). The data set comes from an original (non-machine-learning) study (Nash et al., 1994). It has 4177 examples, and the goal is to predict the age of abalone from physical measurements; the names of these measurements are in Figure 7. The age of abalone is determined by counting the number of rings (**Rings**) through a microscope, and this is a time-consuming task. Other physical measurements that are easier to obtain, are used to predict the age. **Rings** can be regarded either as a continuous variable or an ordinal

Simulation setting	Model	RMSE	OOSLLK
1	Linear Regression	9.91	-3.71
	Gaussian Copula Regression	9.91	-3.71
	Vine Copula Regression	9.90	-3.71
2	Linear Regression	11.08	-3.82
	Gaussian Copula Regression	11.13	-3.77
	Vine Copula Regression	11.08	-3.74
3	Linear Regression	0.73	-1.11
	Quadratic Regression	0.63	-0.95
	Vine Copula Regression	0.64	-0.80

Table 3: Root-mean-square error (RMSE) and out-of-sample log-likelihood (OOSLLK) in different simulation settings.

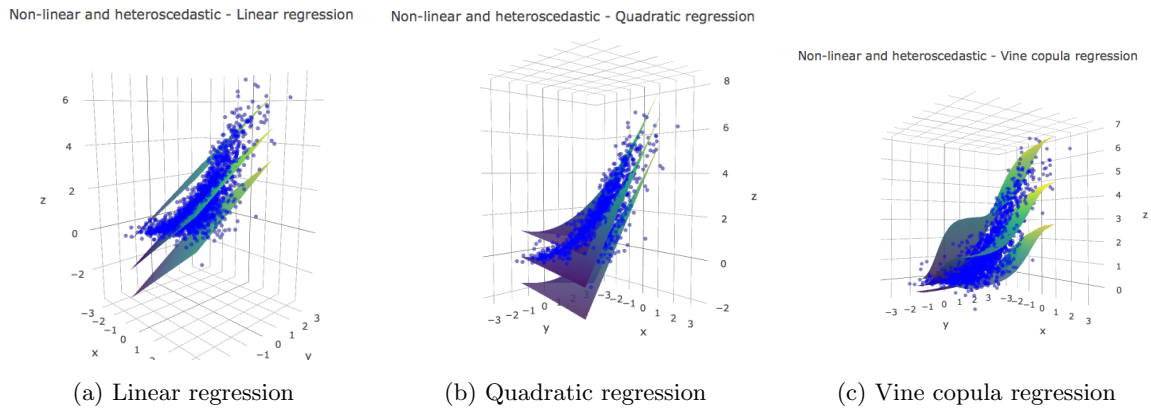


Figure 6: Non-linear and heteroscedastic simulation setting.

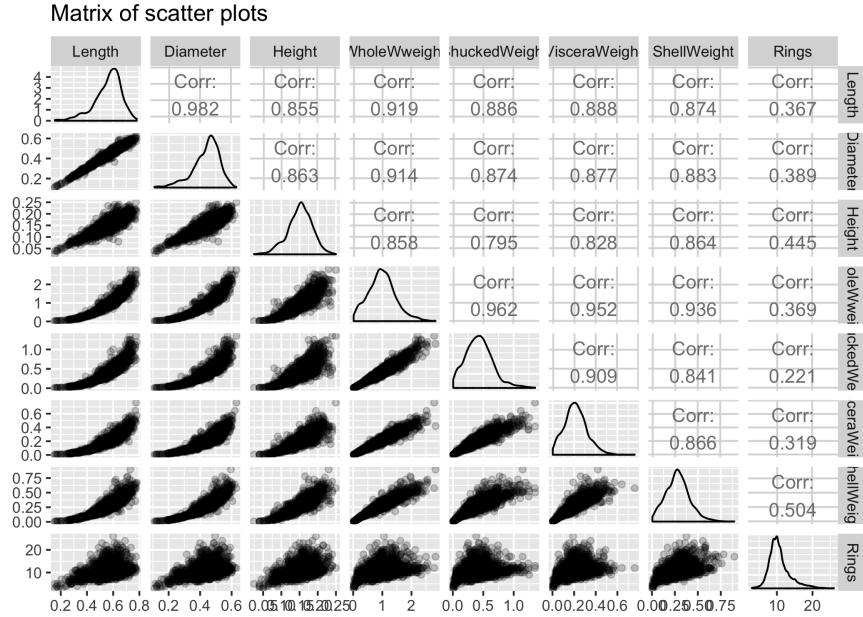


Figure 7: Pairwise scatter plots of the Abalone dataset.

one. Thus the problem can be either a regression or a classification problem. We focus on the subset of 1526 male samples (with two outliers removed). Figure 7 shows the pairwise scatter plots, marginal density functions and pairwise correlation coefficients. There is clear non-linearity and heteroscedasticity among the pairs of variables. We discuss the regression problem in Section 6.2, and Section 6.3 shows the results for the classification problem.

6.2 Regression

In this section, we compare the performance of vine copula and linear regression methods. Three vine regressions are considered:

- R-vine copula regression: the proposed method with the candidate bivariate copula families;
- Gaussian copula regression with R-vine partial correlation parametrization: the proposed method with the bivariate Gaussian copulas only;
- D-vine copula regression: Kraus and Czado (2017) with the candidate bivariate copula families.

The candidate bivariate copulas include Student- t , MTCJ, Gumbel, Frank, Joe, BB1, BB6, BB7, and the corresponding survival and reflected copulas.

The data set is randomly partitioned into a training set (80%) and a test set (20%). Vine copula regressions and linear regression are fitted using the training set, and the test set is used for performance evaluation. All the univariate margins are fitted by skew-normal distributions. The conditional mean and 95% prediction interval are obtained for the test set. For copula regressions, the upper and lower bounds of the 95% prediction interval are the conditional 97.5% and 2.5% quantiles respectively.

We consider four out-of-sample performance measures:

- Root-mean-square error: the square root of the mean squared prediction error.
- Median absolute error: the median of the absolute prediction error.
- Mean interval length: the average length of the prediction intervals.
- Coverage proportion: the proportion of the prediction intervals that covers the true value. We expect the coverage proportion to be at least 95%.

	R-vine copula	Gaussian copula	D-vine copula	Linear reg.
Root-mean-square error	2.191	2.354	2.234	2.351
Median absolute error	1.159	1.303	1.161	1.258
Mean interval length	8.223	8.264	8.234	8.829
Coverage proportion	0.958	0.931	0.961	0.941
OOSLLK	-2.052	-2.163	-2.063	-2.273

Table 4: Comparison of the performance of vine copula regressions and linear regression on the test set.

4 4 4 4 4 7 1 7	-	BB6.s	BB6.s	BB6.s	Gumbel.s	Gumbel.s	BB6.s	Gumbel.s
7 7 7 5 4 4 4	-	-	t	Joe.v	BB8.s	t	Frank	BB8.u
5 5 7 6 5 5	-	-	-	t	Frank	t	BB8.v	BB8.u
6 6 5 7 6	-	-	-	-	BB8	Gauss	Frank	MTCJ.v
1 1 6 3	-	-	-	-	-	t	Frank	t
3 3 1	-	-	-	-	-	-	Gumbel	t
2 2	-	-	-	-	-	-	-	Gumbel.u
8	-	-	-	-	-	-	-	-

Table 5: Vine array and bivariate copulas of the R-vine copula regression. The variables are (1) **Length**, (2) **Diameter**, (3) **Height**, (4) **WholeWeight**, (5) **ShuckedWeight**, (6) **VisceraWeight**, (7) **ShellWeight**, (8) **Rings**. A suffix of ‘s’ represents survival version of the copula family to get the opposite direction of joint tail asymmetry; ‘u’ and ‘v’ represent the copula family with reflection on the first and second variable respectively to get negative dependence.

Table 4 shows the performance measures on the test set. Compared with linear regression, our method has lower prediction errors, and narrower prediction intervals with the expected coverage proportion. The vine array and bivariate copulas on the edges of the R-vine are shown in Table 5. Several of the copulas linking to the response variables in trees 2 to 7 represent weak negative dependence.

We have also conducted monotonicity checks of the predicted conditional median based on the fitted R-vine model. Four of the linking copulas in trees 2 to 7 (last column of the right-hand side of Table 5) represent conditional negative dependence given the previously linked variables to the response variable. This means that the conditional median function is not always monotone increasing in an explanatory variable when others are held fixed. However, when all explanatory variables are increasing together (for larger abalone), the conditional median is increasing. This property is similar to classical Gaussian regression with positive correlated explanatory variables and existence of negative regression coefficients because of some negative partial correlations. Even with some negative conditional dependence, there is overall better out-of-sample prediction performance by keeping all of the explanatory variables in the model.

We also did some numerical checks on the conditional quantiles when one explanatory variable becomes extreme and other variables are held fixed. It appears that the behavior is close to asymptotically constant. From the linking copulas in Table 5 and the results in Section 4, we would not be expecting asymptotic linear behavior (and this is reasonable from the context of the variables).

The fitted D-vine regression model has path

$$\text{VisceraWeight} - \text{WholeWeight} - \text{ShuckedWeight} - \text{ShellWeight} - \text{Rings}$$

in the first level of the D-vine structure.

Figure 8 visualizes the prediction performance of the three methods. The plots show the residuals against the fitted values on the test set, and the prediction intervals. Due to heteroscedasticity, there is more variation in residuals as fitted value increases. However, linear regression fails to capture the heteroscedasticity and the prediction intervals are roughly of the same length. Vine copula regression gives wider (narrower) prediction intervals when the fitted values are larger (smaller). This illustrates the reason why our method overall has more precise prediction intervals.

In Appendix G, further analysis is done to compare the four methods to show where they differ the most in terms of point predictions. The largest differences are when samples are near the upper boundary of the

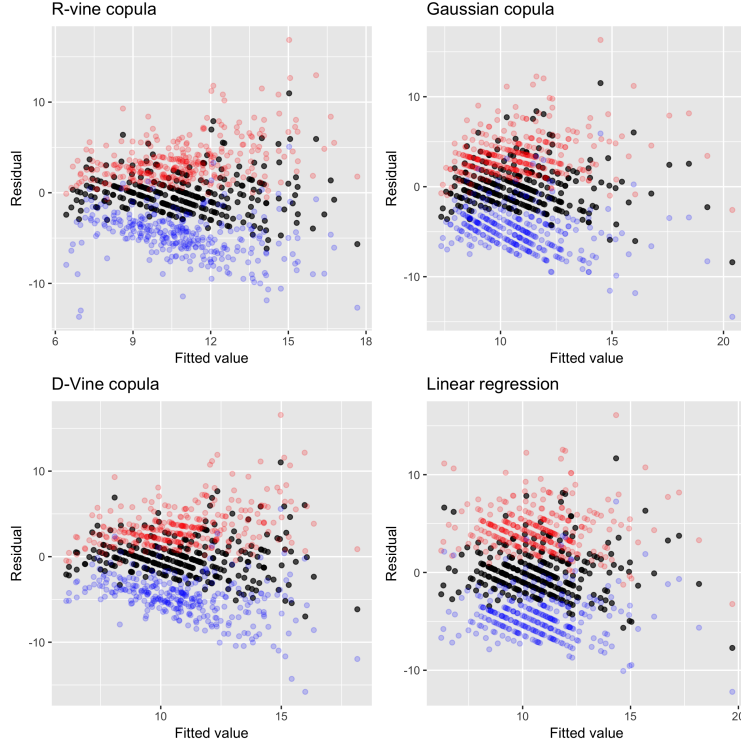


Figure 8: Residual vs. fitted value plots. The red and blue points are the upper bound and lower bound of the prediction intervals.

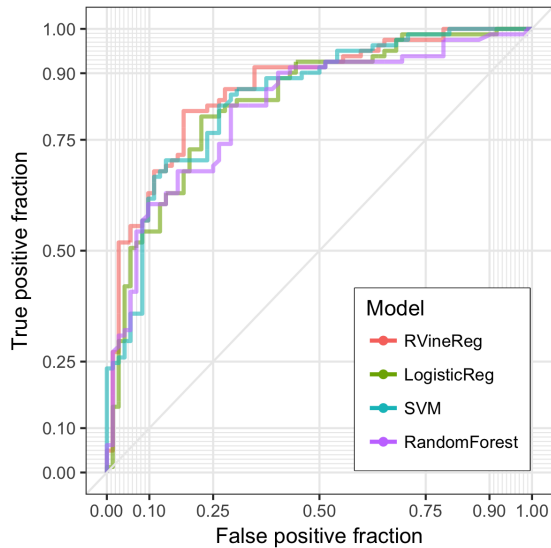
predictor space; that is, at least one of the predictor variables is above its 95th quantile. This is an indication that R-vine copula and D-vine copula models are more flexible than Gaussian copula and linear regression models in handling tail behaviors.

6.3 Classification

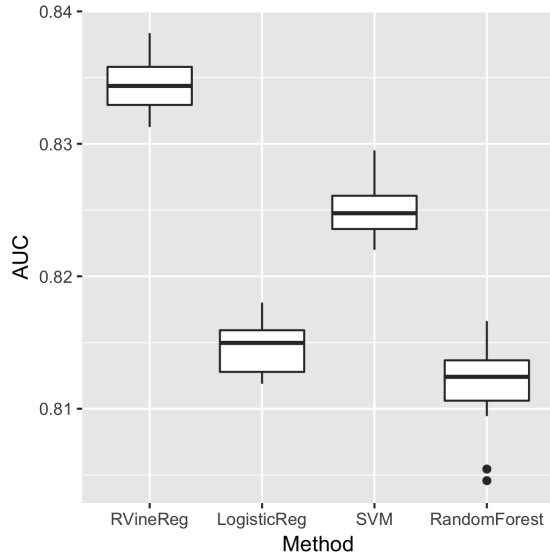
The response variable `Rings` is an ordinal variable that ranges from 3 to 27. Therefore this is a multiclass classification problem. Although our method can handle multiclass classification problems, we reduce it to a binary classification problem for easy comparison with commonly used methods, including logistic regression, support vector machine (SVM), and random forest. The sample median of `Rings` is 10; if a sample's `Rings` is greater than 10, we label it as 'large', otherwise 'small'. All the predictor variables are fitted by skew-normal distributions, and we fit an empirical distribution to the response variable `Rings`.

For binary classifiers, the performance can be demonstrated by a receiver operating characteristic (ROC) curve. The curve is created by plotting the true positive rate against the false positive rate at various threshold settings. The (0, 1) point corresponds to a perfect classification; a completely random guess would give a point along the diagonal line. An ROC curve is a two-dimensional depiction of classifier performance. To compare classifiers we may want to reduce ROC performance to a scalar value representing the expected performance. A common method is to calculate the area under the ROC curve, abbreviated AUC (Fawcett, 2006). The AUC can also be interpreted as the probability that a classifier will rank a randomly chosen positive instance higher than a randomly chosen negative one. Therefore, larger AUC is better. Figure 9a shows sample ROC curves of different binary classifiers and the corresponding AUCs. The AUCs are: CopulaReg = 0.861, LogisticReg = 0.836, SVM = 0.844, RandomForest = 0.823.

Repeated 10-fold cross validations with random partitions is used to assess the performance. In each pass, a 10-fold cross validation is performed and the average AUC is recorded. Figure 9b shows a box plot of the average AUCs. The performance of vine copula regression is marginally but significantly better than the other methods.



(a) ROC curves of different binary classifiers. The performance is evaluated on the test set.



(b) Box plot of the AUCs based on 10-fold cross validations, repeated 20 times.

Figure 9: Comparison of the performance on the classification problem.

7 Conclusion

In this paper, a novel vine copula regression method is proposed. Compared to the existing methods that either use D-vines or only handle continuous variables, the proposed method uses R-vines and can fit mixed continuous and ordinal variables. The prediction algorithm can efficiently compute the conditional distribution given a fitted vine copula, without marginalizing the conditioning variables.

To relate how choices of bivariate copula families in the vine can affect prediction and to provide guidelines on bivariate copula families to consider, we give a theoretical analysis on the asymptotic shape of conditional quantile functions. For bivariate copulas, the conditional quantile function of the response variable could be asymptotically linear, sublinear, or constant with respect to the explanatory variable. It turns out the asymptotic conditional distribution can be quite complex for trivariate and higher-dimensional cases, and there are counter-intuitive examples. In practice, we recommend some plots of conditional quantile functions of the fitted vine copula to assess if the monotonicity properties are reasonable.

The performance of the proposed method is evaluated on simulated data sets and the Abalone data set. The heteroscedasticity in the data is better captured by vine copula regression than the standard regression methods.

Acknowledgements

This research has been supported by an NSERC Discovery Grant 8698, and a Collaborative Research Team grant for the project: *Copula Dependence Modeling: Theory and Applications* of the Canadian Statistical Sciences Institute.

References

- Aas, K., Czado, C., Frigessi, A., and Bakken, H. (2009). Pair-copula constructions of multiple dependence. *Insurance: Mathematics and Economics*, 44(2):182–198.
- Abramowitz, M. and Stegun, I. A. (1964). *Handbook of mathematical functions: with formulas, graphs, and mathematical tables*, volume 55. Courier Corporation.

- Bedford, T. and Cooke, R. M. (2001). Probability density decomposition for conditionally dependent random variables modeled by vines. *Annals of Mathematics and Artificial Intelligence*, 32(1-4):245–268.
- Bedford, T. and Cooke, R. M. (2002). Vines — a new graphical model for dependent random variables. *Annals of Statistics*, 30(4):1031–1068.
- Bernard, C. and Czado, C. (2015). Conditional quantiles and tail dependence. *Journal of Multivariate Analysis*, 138:104–126.
- Brechmann, E. C., Czado, C., and Aas, K. (2012). Truncated regular vines in high dimensions with application to financial data. *Canadian Journal of Statistics*, 40(1):68–85.
- Brechmann, E. C. and Joe, H. (2014). Parsimonious parameterization of correlation matrices using truncated vines and factor analysis. *Computational Statistics & Data Analysis*, 77:233–251.
- Cooke, R. M., Joe, H., and Chang, B. (2015). Vine regression. *Resources for the Future Discussion Paper*, 15-52.
- Dissmann, J., Brechmann, E. C., Czado, C., and Kurowicka, D. (2013). Selecting and estimating regular vine copulae and application to financial returns. *Computational Statistics & Data Analysis*, 59:52–69.
- Fawcett, T. (2006). An introduction to roc analysis. *Pattern Recogn. Lett.*, 27(8):861–874.
- Hastie, T., Tibshirani, R., and Friedman, J. (2009). *The elements of statistical learning: data mining, inference and prediction*. Springer, 2 edition.
- Hua, L. and Joe, H. (2011). Tail order and intermediate tail dependence of multivariate copulas. *Journal of Multivariate Analysis*, 102(10):1454–1471.
- Joe, H. (2014). *Dependence modeling with copulas*. Chapman & Hall/ CRC, Boca Raton, FL.
- Kraus, D. and Czado, C. (2017). D-vine copula based quantile regression. *Computational Statistics & Data Analysis*, 110:1–18.
- Kurowicka, D. and Joe, H. (2011). *Dependence Modeling: Vine Copula Handbook*. World Scientific, Singapore.
- Lichman, M. (2013). UCI machine learning repository.
- Nash, W. J., Sellers, T. L., Talbot, S. R., Cawthorn, A. J., and Ford, W. B. (1994). The population biology of abalone (*Haliotis* species) in tasmania. i. blacklip abalone (*H. rubra*) from the north coast and islands of bass strait. *Sea Fisheries Division, Technical Report*, (48).
- Parsa, R. A. and Klugman, S. A. (2011). Copula regression. *Variance Advancing and Science of Risk*, 5:45–54.
- Schallhorn, N., Kraus, D., Nagler, T., and Czado, C. (2017). D-vine quantile regression with discrete variables. *arXiv preprint arXiv:1705.08310*.
- Sklar, A. (1959). Fonctions de répartition à n dimensions et leurs marges. *Publications de l'Institut de Statistique de l'Université de Paris*, 8:229–231.
- Stöber, J., Hong, H. G., Czado, C., and Ghosh, P. (2015). Comorbidity of chronic diseases in the elderly: Patterns identified by a copula design for mixed responses. *Computational Statistics and Data Analysis*, 88:28–39.

A Vine array representation

An R-vine can be represented by the edge sets at each level $E(T_\ell)$, or equivalently by a graph, such as Figure 10. But those representations are not convenient; we need a more compact way to represent vine models. A vine array $A = (a_{jk})$ for a regular vine $\mathcal{V} = (T_1, \dots, T_{d-1})$ on d elements is a $d \times d$ upper triangular matrix. There is an ordering of the variable indexes along the diagonal, and row ℓ , column j shows the variable $a_{\ell j}$ is connected to the variable $a_{\ell \ell}$ in tree ℓ , conditioning on variables $a_{1j}, \dots, a_{\ell-1,j}$. That is, the first ℓ rows of A and the diagonal elements encode the ℓ -th tree T_ℓ , such that $[a_{\ell j}, a_{jj} | a_{1j}, \dots, a_{\ell-1,j}] \in E(T_\ell)$, for $\ell + 1 \leq j \leq d$. For example, the vine array A_1 represents the R-vine in Figure 10. The edges of T_1 include $[a_{12}, a_{22}] = [23]$, $[a_{13}, a_{33}] = [24]$, $[a_{14}, a_{44}] = [21]$, $[a_{15}, a_{55}] = [35]$. The edges of T_2 include $[a_{23}, a_{33} | a_{13}] = [34|2]$, $[a_{24}, a_{44} | a_{14}] = [31|2]$, $[a_{25}, a_{55} | a_{15}] = [25|3]$.

$$A_1 = \begin{pmatrix} 2 & 2 & 2 & 2 & 3 \\ & 3 & 3 & 3 & 2 \\ & & 4 & 4 & 4 \\ & & & 1 & 1 \\ & & & & 5 \end{pmatrix}, \quad A_2 = \begin{pmatrix} 2 & 2 & 2 & 3 & 2 \\ & 3 & 3 & 2 & 3 \\ & & 4 & 4 & 4 \\ & & & 5 & 5 \\ & & & & 1 \end{pmatrix}.$$

Note that a valid vine array represent a unique R-vine. However, a R-vine may have multiple vine array representations. For example, A_1 and A_2 encode exactly the same R-vine. In real application, the variables are labeled arbitrarily. We can define a permutation of the variables so that the diagonal elements are $(1, 2, \dots, d)$. Therefore, Algorithm 3.1 only applies to vine arrays with ordered diagonal elements.

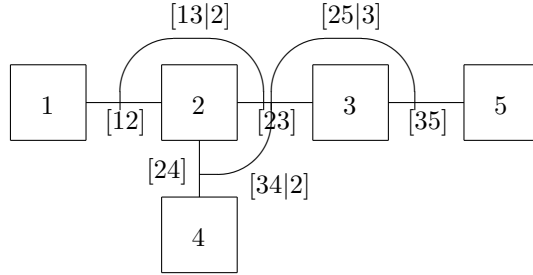


Figure 10: First two trees T_1 and T_2 of a vine \mathcal{V} . The node set and edge set of T_1 are $N(T_1) = \{1, 2, 3, 4, 5\}$ and $E(T_1) = \{[12], [23], [24], [35]\}$. The node set and edge set of T_2 are $N(T_2) = E(T_1) = \{[12], [23], [24], [35]\}$ and $E(T_2) = \{[13|2], [25|3], [34|2]\}$.

B Proof of Proposition 4.1

For the proof, we use the following asymptotic results from Abramowitz and Stegun (1964).

$$\Phi(z) \sim 1 - \frac{\phi(z)}{z} \sim 1 - \frac{1}{\sqrt{2\pi}z} e^{-z^2/2}, \quad z \rightarrow +\infty; \quad \Phi^{-1}(p) \sim (-2 \log(1-p))^{1/2}, \quad p \rightarrow 1^-.$$

$$\Phi(z) \sim -\frac{\phi(z)}{z} \sim \frac{1}{\sqrt{2\pi}|z|} e^{-z^2/2}, \quad z \rightarrow -\infty; \quad \Phi^{-1}(p) \sim -(-2 \log p)^{1/2}, \quad p \rightarrow 0^+.$$

Proof. Using the notation above

$$\Phi^{-1}(C_{V|U}^{-1}(\alpha|u)) \sim -(-2 \log C_{V|U}^{-1}(\alpha|u))^{1/2} \sim -(2k_\alpha(-\log u)^\eta)^{1/2}. \quad (\text{B.1})$$

When $u = \Phi(x) \sim \phi(x)/|x|$,

$$-\log u \sim -\log \phi(x) + \log |x| \sim \frac{1}{2}x^2 + \log |x| \sim \frac{1}{2}x^2. \quad (\text{B.2})$$

Combining (B.1) and (B.2), we obtain the asymptotic conditional quantile function as $x \rightarrow -\infty$,

$$F_{Y|X}^{-1}(\alpha|x) = \Phi^{-1}(C_{V|U}^{-1}(\alpha|\Phi(x))) \sim -(2k_\alpha(x^2/2)^\eta)^{1/2} \sim -(2^{1-\eta}k_\alpha)^{1/2}|x|^\eta.$$

The proof of the second part is similar and thus omitted. \square

C Bivariate Archimedean copula boundary conditional distributions

This section includes the proof of Section 4.2, as well as results used in Section 4.2.2. A bivariate Archimedean copula with Laplace transform generator ψ can be constructed as $C(u, v) = \psi(\psi^{-1}(u) + \psi^{-1}(v))$, where $u, v \in [0, 1]$, $\psi(\infty) = 0$, $\psi(0) = 1$, and ψ is non-increasing and convex. It is the CDF of a random vector (U, V) . The corresponding conditional distribution $P(V \leq v|U = u)$ is

$$C_{V|U}(v|u) = \frac{\partial C(u, v)}{\partial u} = \frac{\psi'(\psi^{-1}(u) + \psi^{-1}(v))}{\psi'(\psi^{-1}(u))}.$$

We study the limit of the conditional distribution $C_{V|U}(v|u)$ as $u \rightarrow 0$ (or 1), and v could be a number in $(0, 1)$ or $v \rightarrow 0$ (or 1) as well. The limit depends on the lower (upper) tail behavior of the copula, and the rate at which u and v goes to 0 (or 1). The rate is characterized on the normal scale: we assume $u, v \rightarrow 0$ (or 1) and $\Phi^{-1}(u)/\Phi^{-1}(v)$ converges to a constant. In other words, if $X = \Phi^{-1}(U)$ and $Y = \Phi^{-1}(V)$, we study the conditional distribution $P(Y \leq y|X = x)$ as $x, y \rightarrow +\infty$ (or $-\infty$) and x/y converges to a constant.

C.1 Lower tail

To avoid technicalities, we assume the following from Equation (8.42) of Joe (2014). As $s \rightarrow \infty$,

$$\psi(s) \sim T(s) = a_1 s^q \exp(-a_2 s^r) \quad \text{and} \quad \psi'(s) \sim T'(s), \quad (\text{C.1})$$

where $a_1 > 0$, $r = 0$ implies $a_2 = 0$ and $q < 0$, and $r > 0$ implies $r \leq 1$ and q can be 0, negative or positive.

C.1.1 Lower tail dependence ($r = 0$)

According to Theorem 8.34 in Joe (2014), for a bivariate Archimedean copula, when $r = 0$ and $\psi \in \text{RV}_q$ where $q < 0$, it has lower tail dependence with $\lambda_L = 2^q$. Therefore, $\psi(s) \sim a_1 s^q$, $\psi'(s) \sim a_1 q s^{q-1}$ and $\psi^{-1}(u) \sim (u/a_1)^{1/q}$, as $s \rightarrow \infty$ and $u \rightarrow 0^+$. If $u \rightarrow 0$, $v \in (0, 1)$ and $\alpha \in (0, 1)$, then

$$C_{V|U}(v|u) \sim \left(1 + \frac{\psi^{-1}(v)}{\psi^{-1}(u)}\right)^{q-1} \sim 1 + (q-1)\psi^{-1}(v) \left(\frac{u}{a_1}\right)^{-1/q} \rightarrow 1, \quad (\text{C.2})$$

For the conditional quantile, we set $C_{V|U}(v|u) = \alpha$ and solve for v . As $u \rightarrow 0$, v should also converge to 0, otherwise $C_{V|U}(v|u) \rightarrow 1$. If $u, v \rightarrow 0$, the conditional distribution is asymptotic to

$$C_{V|U}(v|u) \sim \left(1 + \left(\frac{v}{u}\right)^{1/q}\right)^{q-1}, \quad (u, v) \rightarrow (0, 0). \quad (\text{C.3})$$

Therefore,

$$\begin{aligned} \alpha &\sim \left(1 + \frac{\psi^{-1}(v)}{\psi^{-1}(u)}\right)^{q-1} \sim \left(1 + \left(\frac{v}{u}\right)^{1/q}\right)^{q-1}, \\ C_{V|U}^{-1}(\alpha|u) &\sim \left(\alpha^{1/(q-1)} - 1\right)^q \cdot u \rightarrow 0. \end{aligned}$$

(The above is one result in Proposition 4.2.) If we further assume $u \sim v^k$, where $k \in (0, \infty)$, then

$$C_{V|U}(v|u) \sim \left(1 + u^{(1/k-1)/q}\right)^{q-1}, \quad (u, v) \rightarrow (0, 0), \quad u \sim v^k.$$

Depending on the value of k , there are three different cases:

$$C_{V|U}(v|u) \sim \begin{cases} 1 + (q-1)u^{(1/k-1)/q} \rightarrow 1 & \text{if } k > 1, \\ 2^{q-1} \in (0, 1) & \text{if } k = 1, \\ u^{\frac{q-1}{q}(\frac{1}{k}-1)} \rightarrow 0 & \text{if } 0 < k < 1. \end{cases} \quad (\text{C.4})$$

C.1.2 Lower tail intermediate dependence ($0 < r < 1$)

If $0 < r < 1$, then $C(u, v)$ has lower tail intermediate dependence with $1 < \kappa_L(C) = 2^r < 2$ (Hua and Joe, 2011). $\psi'(s) \sim -a_1 a_2 r s^{q+r-1} \exp(-a_2 s^r)$ and $\psi^{-1}(u) \sim (-\log u/a_2)^{1/r}$, as $s \rightarrow \infty$ and $u \rightarrow 0$.

$$\begin{aligned} C_{V|U}(v|u) &\sim \frac{(\psi^{-1}(u) + \psi^{-1}(v))^{q+r-1} \exp(-a_2 (\psi^{-1}(u) + \psi^{-1}(v))^r)}{(\psi^{-1}(u))^{q+r-1} \exp(-a_2 (\psi^{-1}(u))^r)} \\ &\sim \left(1 + \frac{\psi^{-1}(v)}{\psi^{-1}(u)}\right)^{q+r-1} \exp\left\{-a_2 (\psi^{-1}(u))^r \left[\left(1 + \frac{\psi^{-1}(v)}{\psi^{-1}(u)}\right)^r - 1\right]\right\}, \quad u \rightarrow 0. \end{aligned} \quad (\text{C.5})$$

If $v \in (0, 1)$ is fixed, then as $u \rightarrow 0$,

$$\begin{aligned} C_{V|U}(v|u) &\sim \left(1 + (q+r-1)\frac{\psi^{-1}(v)}{\psi^{-1}(u)}\right) \exp(-a_2 r \psi^{-1}(v) (\psi^{-1}(u))^{r-1}) \\ &\sim \left(1 + (q+r-1)\frac{\psi^{-1}(v)}{\psi^{-1}(u)}\right) \left(1 - a_2 r \psi^{-1}(v) (\psi^{-1}(u))^{r-1}\right) \\ &\sim 1 - a_2 r \psi^{-1}(v) (\psi^{-1}(u))^{r-1} \\ &\sim 1 - a_2^{1/r} r \psi^{-1}(v) (-\log u)^{1-1/r} \rightarrow 1, \quad u \rightarrow 0, \quad v \in (0, 1) \text{ fixed}. \end{aligned} \quad (\text{C.6})$$

For the conditional quantile, we set $C_{V|U}(v|u) = \alpha \in (0, 1)$ and solve for v . According to (C.5), if $\psi^{-1}(v)/\psi^{-1}(u)$ does not converge to 0, then $C_{V|U}(v|u) \rightarrow 0$. It must be that $\psi^{-1}(v)/\psi^{-1}(u) \rightarrow 0$ and

$$C_{V|U}(v|u) \sim \exp(-a_2 r \psi^{-1}(v) (\psi^{-1}(u))^{r-1}) \sim \alpha.$$

Solving for v , we have

$$C_{V|U}^{-1}(\alpha|u) \sim \exp\left[-\left(\frac{-\log \alpha}{r}\right)^r (-\log u)^{1-r}\right] \rightarrow 0, \quad u \rightarrow 0.$$

(The above is one result in Proposition 4.2.) If $u, v \rightarrow 0$, the conditional distribution is asymptotic to

$$C_{V|U}(v|u) \sim \left(1 + \left(\frac{-\log v}{-\log u}\right)^{1/r}\right)^{q+r-1} \exp\left(-(-\log u) \left(1 + \left(\frac{-\log v}{-\log u}\right)^{1/r}\right)^r + (-\log u)\right), \quad (u, v) \rightarrow (0, 0). \quad (\text{C.7})$$

If we further assume $u \sim v^k$, where $k \in (0, \infty)$, then

$$C_{V|U}(v|u) \sim \left(1 + \left(\frac{1}{k}\right)^{1/r}\right)^{q+r-1} u^{(1+(1/k)^{1/r})^r - 1} \rightarrow 0, \quad (\text{C.8})$$

regardless of the value of k .

C.1.3 Lower tail quadrant independence ($r = 1$)

If $r = 1$, then the copula has $\kappa_L = 2$ and $\text{support}(C_{V|U}(\cdot|0)) = (0, 1)$. Therefore $\lim_{u \rightarrow 0} C_{V|U}(v|u) \in (0, 1)$ if $v \in (0, 1)$, and $C_{V|U}(v|u) \rightarrow 0$ if $(u, v) \rightarrow (0, 0)$.

C.2 Upper tail

(Proposition 3 in Hua and Joe (2011)) Suppose $\psi(s)$ is the Laplace transform (LT) of a positive variable Y with $k < M < k + 1$ where $M = \sup\{m \geq 0 : \mathbb{E}(Y^m) < \infty\}$ and $k \in \{0\} \cup \mathbb{N}_+$. If $|\psi^{(k)} - \psi^{(k)}(s)|$ is regularly varying at 0^+ , then $|\psi^{(k)} - \psi^{(k)}(s)| \in \mathcal{R}_{M-k}(0^+)$. In particular, if the slowly varying component is $\ell(s)$ and $\lim_{s \rightarrow 0^+} \ell(s) = h^{k+1}$ with $0 < h^{k+1} < \infty$, then

$$\psi(s) = \sum_{i=0}^k (-1)^i h_i s^i + (-1)^{k+1} h_{k+1} s^M + o(s^M), \quad s \rightarrow 0^+, \quad (\text{C.9})$$

where $h_0 = 1$ and $0 < h_i < \infty$ for $i = 1, \dots, k + 1$. If $0 < M < 1$, then $k = 0$.

C.2.1 Upper tail dependence ($0 < M < 1$)

By Proposition 4 in Hua and Joe (2011), if $0 < M < 1$, then $C(u, v)$ has upper tail dependence with $\lambda_U = 2 - 2^M$. In this case, $\psi(s)$ can be written as $\psi(s) \sim 1 - h_1 s^M$, as $s \rightarrow 0^+$, where $0 < h_1 < \infty$ and $0 < M < 1$. Therefore, $\psi'(s) \sim -h_1 M s^{M-1}$,

$$\psi^{-1}(u) \sim \left(\frac{1-u}{h_1} \right)^{1/M}, \quad u \rightarrow 1.$$

If $v \in (0, 1)$ and $\alpha \in (0, 1)$ are fixed, then as $u \rightarrow 1$,

$$C_{V|U}(v|u) \sim -\frac{\psi'(\psi^{-1}(v))}{h_1^{1/M} M} (1-u)^{(1-M)/M} \rightarrow 0. \quad (\text{C.10})$$

For the conditional quantile, we set $C_{V|U}(v|u) = \alpha \in (0, 1)$ and solve for v . Since $C_{V|U}(v|u) = \psi'(\psi^{-1}(u) + \psi^{-1}(v))/\psi'(\psi^{-1}(u))$, if v does not converge to 1, then $C_{V|U}(v|u) \rightarrow 0$. Therefore, we have $(u, v) \rightarrow (1, 1)$ and the conditional distribution is asymptotic to

$$C_{V|U}(v|u) \sim \left(1 + \left(\frac{1-v}{1-u} \right)^{1/M} \right)^{M-1}. \quad (\text{C.11})$$

Solving for v , the conditional quantile function is

$$C_{V|U}^{-1}(\alpha|u) \sim 1 - \left(\alpha^{1/(M-1)} - 1 \right)^M (1-u) \rightarrow 1, \quad u \rightarrow 1.$$

(The above is one result in Proposition 4.2.) If we further assume $(1-u) \sim (1-v)^k$, where $k \in (0, \infty)$, then

$$C_{V|U}(v|u) \sim \left(1 + (1-u)^{(1/k-1)/M} \right)^{M-1}, \quad u \rightarrow 1. \quad (\text{C.12})$$

Depending on the value of k , there are three different cases:

$$C_{V|U}(v|u) \sim \begin{cases} (1-u)^{(M-1)(1/k-1)/M} \rightarrow 0 & \text{if } k > 1, \\ 2^{M-1} \in (0, 1) & \text{if } k = 1, \\ 1 + (M-1)(1-u)^{(1/k-1)/M} \rightarrow 1 & \text{if } 0 < k < 1. \end{cases} \quad (\text{C.13})$$

C.2.2 Upper tail intermediate dependence / quadrant independence ($M > 1$)

By Proposition 7 in Hua and Joe (2011), if $M > 1$, then the copula C has upper tail intermediate dependence or independence, and $\text{support}(C_{V|U}(\cdot|1)) = (0, 1)$. Therefore, $\lim_{u \rightarrow 1} C_{V|U}(v|u) \in (0, 1)$ if $v \in (0, 1)$, and $C_{V|U}(v|u) \rightarrow 1$ if $(u, v) \rightarrow (1, 1)$.

D Derivations for Section 4.2.1

Tail expansions of the gamma CDF

For a random variable Z following $\text{Gamma}(\alpha, \beta)$, the CDF is $F_Z(z) = \gamma(\alpha, \beta z)/\Gamma(\alpha)$, where $\gamma(\cdot, \cdot)$ is the lower incomplete gamma function. Its CDF F_Z and quantile function F_Z^{-1} have the following asymptotic behavior:

$$F_Z(z) \sim 1 - \frac{(\beta z)^{\alpha-1}}{\Gamma(\alpha)} e^{-\beta z}, \quad z \rightarrow +\infty; \quad F_Z^{-1}(p) \sim -\frac{\log(1-p)}{\beta}, \quad p \rightarrow 1^-.$$

$$F_Z(z) \sim \frac{(\beta z)^\alpha}{\Gamma(\alpha+1)}, \quad z \rightarrow 0^+; \quad F_Z^{-1}(p) \sim \frac{p^{1/\alpha} \Gamma(\alpha+1)^{1/\alpha}}{\beta}, \quad p \rightarrow 0^+.$$

Upper tail

We first study the upper tail asymptotic behavior of $g(x_1, x_2)$ as $x_1, x_2 \rightarrow +\infty$.

$$\Phi(x_1) \sim 1 - \frac{1}{\sqrt{2\pi}x_1} e^{-x_1^2/2}, \quad x_1 \rightarrow +\infty,$$

$$F_{X_1^*}^{-1}(\Phi(x_1)) \sim -\log\left(\frac{1}{\sqrt{2\pi}x_1} e^{-x_1^2/2}\right) \sim \frac{x_1^2}{2}, \quad x_1 \rightarrow +\infty.$$

Similarly,

$$F_{X_2^*}^{-1}(\Phi(x_2)) \sim \frac{x_2^2}{2}, \quad x_2 \rightarrow +\infty.$$

$$F_{Y^*}\left(F_{X_1^*}^{-1}(\Phi(x_1)) + F_{X_2^*}^{-1}(\Phi(x_2))\right) \sim 1 - \frac{1}{\Gamma(\alpha_1 + \alpha_2)} \left(\frac{(x_1^2 + x_2^2)^{\alpha_1 + \alpha_2 - 1}}{2}\right) e^{-(x_1^2 + x_2^2)/2}, \quad x_1, x_2 \rightarrow +\infty.$$

Finally,

$$g(x_1, x_2) = \Phi^{-1}\left(F_{Y^*}\left(F_{X_1^*}^{-1}(\Phi(x_1)) + F_{X_2^*}^{-1}(\Phi(x_2))\right)\right)$$

$$\sim \left(-2 \log\left(1 - F_{Y^*}\left(F_{X_1^*}^{-1}(\Phi(x_1)) + F_{X_2^*}^{-1}(\Phi(x_2))\right)\right)\right)^{1/2}$$

$$\sim (x_1^2 + x_2^2)^{1/2}, \quad x_1, x_2 \rightarrow +\infty.$$

If $x_2 \sim kx_1$ as $x_1, x_2 \rightarrow +\infty$, then $g(x_1, x_2) \sim \sqrt{1+k^2}x_1$.

Lower tail

For the lower tail, $x_1, x_2 \rightarrow -\infty$,

$$\Phi(x_1) \sim -\frac{1}{\sqrt{2\pi}x_1} e^{-x_1^2/2}, \quad x_1 \rightarrow -\infty,$$

and

$$F_{X_1^*}^{-1}(\Phi(x_1)) \sim \Gamma(\alpha_1 + 1)^{1/\alpha_1} (\Phi(x_1))^{1/\alpha_1} \sim \left(\frac{\Gamma(\alpha_1 + 1)}{\sqrt{2\pi}}\right)^{1/\alpha_1} \left(-\frac{1}{x_1}\right)^{1/\alpha_1} \exp\left(-\frac{x_1^2}{2\alpha_1}\right), \quad x_1 \rightarrow -\infty.$$

Similarly,

$$F_{X_2^*}^{-1}(\Phi(x_2)) \sim \left(\frac{\Gamma(\alpha_2 + 1)}{\sqrt{2\pi}}\right)^{1/\alpha_2} \left(-\frac{1}{x_2}\right)^{1/\alpha_2} \exp\left(-\frac{x_2^2}{2\alpha_2}\right), \quad x_2 \rightarrow -\infty.$$

$$F_{Y^*}\left(F_{X_1^*}^{-1}(\Phi(x_1)) + F_{X_2^*}^{-1}(\Phi(x_2))\right) \sim \frac{1}{\Gamma(\alpha_1 + \alpha_2 + 1)} \left[\left(\frac{\Gamma(\alpha_1 + 1)}{\sqrt{2\pi}}\right)^{1/\alpha_1} \left(-\frac{1}{x_1}\right)^{1/\alpha_1} \exp\left(-\frac{x_1^2}{2\alpha_1}\right) \right. \\ \left. + \left(\frac{\Gamma(\alpha_2 + 1)}{\sqrt{2\pi}}\right)^{1/\alpha_2} \left(-\frac{1}{x_2}\right)^{1/\alpha_2} \exp\left(-\frac{x_2^2}{2\alpha_2}\right) \right]^{\alpha_1 + \alpha_2}.$$

Assuming $x_2 \sim kx_1$, if $k^2 > \alpha_2/\alpha_1$, then $\exp(-x_1^2/(2\alpha_1))$ dominates $\exp(-x_2^2/(2\alpha_2))$.

$$F_{Y^*} \left(F_{X_1^*}^{-1}(\Phi(x_1)) + F_{X_2^*}^{-1}(\Phi(x_2)) \right) = O \left(\left(-\frac{1}{x_1} \right)^{(\alpha_1+\alpha_2)/\alpha_1} \exp \left(-\frac{(\alpha_1+\alpha_2)x_1^2}{2\alpha_1} \right) \right),$$

and

$$\begin{aligned} g(x_1, x_2) &= \Phi^{-1} \left(F_{Y^*} \left(F_{X_1^*}^{-1}(\Phi(x_1)) + F_{X_2^*}^{-1}(\Phi(x_2)) \right) \right) \\ &\sim \left(-2 \log \left(F_{Y^*} \left(F_{X_1^*}^{-1}(\Phi(x_1)) + F_{X_2^*}^{-1}(\Phi(x_2)) \right) \right) \right)^{1/2} \\ &\sim \sqrt{\frac{\alpha_1 + \alpha_2}{\alpha_1}} x_1, \quad x_1, x_2 \rightarrow -\infty, x_2 \sim kx_1. \end{aligned}$$

It can be shown that the result holds for $k^2 = \alpha_2/\alpha_1$ as well. Similarly, if $k^2 < \alpha_2/\alpha_1$, then

$$g(x_1, x_2) \sim \sqrt{\frac{\alpha_1 + \alpha_2}{\alpha_2}} kx_1, \quad x_1, x_2 \rightarrow -\infty, x_2 \sim kx_1.$$

In summary,

$$g(x_1, x_2) \sim \begin{cases} \sqrt{\frac{\alpha_1 + \alpha_2}{\alpha_1}} x_1 & \text{if } k^2 \geq \alpha_2/\alpha_1, \\ \sqrt{\frac{\alpha_1 + \alpha_2}{\alpha_2}} kx_1 & \text{if } k^2 < \alpha_2/\alpha_1. \end{cases}$$

E Derivations for Section 4.2.2

Trivariate vine copula lower tail

Fix $v \in (0, 1)$ and let $u_1, u_2 \rightarrow 0$ with $u_2 \sim u_1^k$. According to (C.2) and (C.6), depending on the tail order of $C_{23}(u_2, u_3)$, there are three cases of the limit of $u_{3|2} = C_{3|2}(v|u_2)$ as $u_2 \rightarrow 0$:

- If C_{23} has $\kappa_{23L} = 1$, then from (C.2),

$$u_{3|2} \sim 1 - A_1(v)u_2^{-1/q_{23}} \rightarrow 1, \quad u_2 \rightarrow 0, v \in (0, 1) \text{ fixed}, A_1(v) > 0, \quad (\text{E.1})$$

where q_{23} is a parameter of the LT ψ_{23} for C_{23} in (4.1).

- If C_{23} has $\kappa_{23L} \in (1, 2)$, then from (C.6),

$$u_{3|2} \sim 1 - A_2(v)(-\log u_2)^{1-1/r_{23}} \rightarrow 1, \quad u_2 \rightarrow 0, v \in (0, 1) \text{ fixed}, A_2(v) > 0, \quad (\text{E.2})$$

where r_{23} is a parameter of the LT ψ_{23} for C_{23} in (4.1).

- If C_{23} has $\kappa_{23L} = 2$, then $\lim_{u_2 \rightarrow 0} u_{3|2} \in (0, 1)$.

Therefore, the limit of $u_{3|2} = C_{3|2}(v|u_2)$ could either be a number in $(0, 1)$, or 1.

All cells in Table 1 are clear except row 3, column 6 (cell *), that is $u_{1|2} \rightarrow 1$, $u_{3|2} \rightarrow 1$ and $C_{13;2}$ has upper tail dependence. In this case, the boundary conditional distribution can be written as

$$C_{3|1;2}(u_{3|2}|u_{1|2}) \sim \left(1 + \left(\frac{1 - u_{3|2}}{1 - u_{1|2}} \right)^{1/M_{13;2}} \right)^{M_{13;2}-1}, \quad (u_{1|2}, u_{3|2}) \rightarrow (1, 1),$$

where $M_{13;2}$ is a parameter of the LT $\psi_{13;2}$ for $C_{13;2}$ and $0 < M_{13;2} < 1$.

According to the analysis in Appendix C.1, $u_{1|2} \rightarrow 1$ implies that C_{12} has lower tail dependence and $u_2 \sim u_1^k$ with $k > 1$. However, C_{23} could have $\kappa_{23L} = 1$ or $\kappa_{23L} \in (1, 2)$.

- If C_{23} has $\kappa_{23L} \in (1, 2)$, then from (C.4) and (C.6),

$$\begin{aligned} 1 - u_{3|2} &\sim A_2(v)(-\log u_2)^{1-1/r_{23}}, \quad u_2 \rightarrow 1, v \in (0, 1) \text{ fixed}, A_2(v) > 0, \\ 1 - u_{1|2} &\sim -(q_{12} - 1)u_2^{(1/k-1)/q_{12}}, \quad (u_1, u_2) \rightarrow (1, 1), u_2 \sim u_1^k, q_{12} < 0, \\ \frac{1 - u_{3|2}}{1 - u_{1|2}} &\sim -\frac{A_2(v)}{q_{12} - 1} \frac{(-\log u_2)^{-(1-r_{23})/r_{23}}}{u_2^{(1/k-1)/q_{12}}} \rightarrow \infty, \end{aligned}$$

where r_{23} and q_{12} are the parameters of ψ_{23} for C_{23} and ψ_{12} for C_{12} respectively. Therefore, $C_{3|1;2}(u_{3|2}|u_{1|2}) \rightarrow 0$.

- If C_{23} has $\kappa_{23L} = 1$, then from (C.2) and (C.4),

$$\begin{aligned} 1 - u_{3|2} &\sim A_1(v)u_2^{-1/q_{23}}, \quad u_2 \rightarrow 1, v \in (0, 1) \text{ fixed}, A_1(v) > 0, \\ 1 - u_{1|2} &\sim -(q_{12} - 1)u_2^{(1/k-1)/q_{12}}, \quad (u_1, u_2) \rightarrow (1, 1), u_2 \sim u_1^k, q_{12} < 0, \\ \frac{1 - u_{3|2}}{1 - u_{1|2}} &\sim -\frac{A_1(v)}{q_{12} - 1} u_2^{-1/q_{23} - (1/k-1)/q_{12}}, \end{aligned}$$

where q_{23} and q_{12} are the parameters of ψ_{23} for C_{23} and ψ_{12} for C_{12} respectively. Therefore,

$$C_{3|1;2}(u_{3|2}|u_{1|2}) \rightarrow \begin{cases} 1 & \text{if } -q_{23}^{-1} - q_{12}^{-1}(k^- - 1) > 0, \\ \text{const} \in (0, 1) & \text{if } -q_{23}^{-1} - q_{12}^{-1}(k^- - 1) = 0, \\ 0 & \text{if } -q_{23}^{-1} - q_{12}^{-1}(k^- - 1) < 0. \end{cases}$$

Trivariate vine copula upper tail

Fix $v \in (0, 1)$ and let $(u_1, u_2) \rightarrow (1, 1)$ with $(1 - u_2) \sim (1 - u_1)^k$. According to (C.10), depending on the tail order of $C_{23}(u_2, u_3)$, there are two cases of the limit of $u_{3|2} = C_{3|2}(v|u_2)$ as $u_2 \rightarrow 1$:

- If $C_{3|2}$ has $\kappa_{23U} = 1$, then from (C.10),

$$u_{3|2} \sim A_3(v)(1 - u_2)^{(1-M_{23})/M_{23}} \rightarrow 0, \quad u_2 \rightarrow 1, v \in (0, 1) \text{ fixed}, A_3(v) > 0, \quad (\text{E.3})$$

where M_{23} is a parameter of the LT ψ_{23} for C_{23} in (4.2).

- If $C_{3|2}$ has $\kappa_{23U} \in (1, 2]$, then $\lim_{u_2 \rightarrow 1} u_{3|2} \in (0, 1)$.

Therefore, the limit of $u_{3|2} = C_{3|2}(v|u_2)$ could either be a number in $(0, 1)$, or 0.

Cell * in Table 2. Since $C_{13;2}$ has $\kappa_{13L} \in (1, 2)$, the conditional distribution can be written as, via (C.7),

$$C_{3|1;2}(u_{3|2}|u_{1|2}) \sim \left(1 + \left(\frac{-\log u_{3|2}}{-\log u_{1|2}}\right)^{1/r_{13;2}}\right)^{q_{13;2} + r_{13;2} - 1} u_{1|2}^{\left(1 + \left(\frac{-\log u_{3|2}}{-\log u_{1|2}}\right)^{1/r_{13;2}}\right)^{r_{13;2}} - 1}, \quad (u_{3|2}, u_{1|2}) \rightarrow (0, 0),$$

where $q_{13;2}$ and $r_{13;2}$ are parameters of the LT $\psi_{13;2}$ for $C_{13;2}$, and $0 < r_{13;2} < 1$. Since C_{23} has $\kappa_{23U} = 1$, then by (C.10),

$$u_{3|2} \sim A_3(v)(1 - u_2)^{(1-M_{23})/M_{23}} \rightarrow 0, \quad u_2 \rightarrow 1, v \in (0, 1) \text{ fixed},$$

and

$$-\log u_{3|2} \sim -\log A_3(v) - \frac{M_{23} - 1}{M_{23}}(-\log(1 - u_2)),$$

where M_{23} is a parameter of the LT ψ_{23} for C_{23} . C_{12} has upper tail dependence and $(1 - u_2) \sim (1 - u_1)^k$, where $k > 1$. We have by (C.13),

$$u_{1|2} \sim (1 - u_2)^{(M_{12}-1)(1/k-1)/M_{12}} \rightarrow 0, \quad (u_1, u_2) \rightarrow (1, 1), (1 - u_2) \sim (1 - u_1)^k,$$

and

$$-\log u_{1|2} \sim \frac{M_{12}-1}{M_{12}} \left(\frac{1}{k}-1\right) (-\log(1-u_2)),$$

where M_{12} is a parameter of the LT ψ_{12} for C_{12} . Therefore,

$$B := \frac{-\log u_{3|2}}{-\log u_{1|2}} \sim \frac{-\frac{M_{23}-1}{M_{23}}}{\frac{M_{12}-1}{M_{12}} \left(\frac{1}{k}-1\right)} > 0,$$

and

$$C_{3|1;2}(u_{3|2}|u_{1|2}) \sim (1+B^{1/r})^{q+r-1} u_{1|2}^{(1+B^{1/r})^r-1} \rightarrow 0, \quad u_{1|2} \rightarrow 0.$$

The cell * converges to 0.

Cell † in Table 2. Since $C_{13;2}$ has lower tail dependence, the conditional distribution can be written as, via (C.3),

$$C_{3|1;2}(u_{3|2}|u_{1|2}) \sim \left(1 + \left(\frac{u_{3|2}}{u_{1|2}}\right)^{1/q_{13;2}}\right)^{q_{13;2}-1}, \quad (u_{3|2}, u_{1|2}) \rightarrow (0, 0),$$

where $q_{13;2}$ is a parameter of the LT $\psi_{13;2}$ for $C_{13;2}$ and $q_{13;2} < 0$, $u_{3|2}$ and $u_{1|2}$ are the same as previous. Therefore,

$$\frac{u_{3|2}}{u_{1|2}} \sim A_3(v)(1-u_2)^{-(M_{23}-1)/M_{23}-(M_{12}-1)(1/k-1)/M_{12}}, \quad (u_{3|2}, u_{1|2}) \rightarrow (0, 0),$$

$$C_{3|1;2}(u_{3|2}|u_{1|2}) \rightarrow \begin{cases} 0 & \text{if } -\frac{M_{23}-1}{M_{23}} - \frac{M_{12}-1}{M_{12}} \left(\frac{1}{k}-1\right) > 0, \\ \text{const} \in (0, 1) & \text{if } -\frac{M_{23}-1}{M_{23}} - \frac{M_{12}-1}{M_{12}} \left(\frac{1}{k}-1\right) = 0, \\ 1 & \text{if } -\frac{M_{23}-1}{M_{23}} - \frac{M_{12}-1}{M_{12}} \left(\frac{1}{k}-1\right) < 0. \end{cases}$$

F Derivations for case 1 in Section 4.2.3

Lower tail

We give a more detailed analysis to derive the rate at which the conditional quantile goes to $-\infty$. Let $(u_1, u_2) \rightarrow (0, 0)$ and $u_2 \sim u_1^k$. We are interested in the conditional quantile $C_{3|12}^{-1}(\alpha|u_1, u_2)$. In other words, we need to find v such that $C_{3|2}(v|u_2) = C_{3|1;2}^{-1}(\alpha|u_{1|2})$. Let $r_{12}, r_{23}, r_{13;2}$ be the parameters of ψ_{12} for C_{12} , ψ_{23} for C_{23} and $\psi_{13;2}$ for $C_{13;2}$ respectively. By (C.8),

$$u_{1|2} \sim \left(1 + \left(\frac{1}{k}\right)^{1/r_{12}}\right)^{q_{12}+r_{12}-1} u_2^{(1+(1/k)^{1/r_{12}})^{r_{12}}-1} \rightarrow 0, \quad -\log u_{1|2} = O(-\log u_2).$$

By (4.4),

$$C_{3|1;2}^{-1}(\alpha|u_{1|2}) \sim \exp \left[- \left(\frac{-\log \alpha}{r_{13;2}} \right)^{r_{13;2}} (-\log u_{1|2})^{1-r_{13;2}} \right],$$

$$-\log C_{3|1;2}^{-1}(\alpha|u_{1|2}) \sim - \left(\frac{-\log \alpha}{r_{13;2}} \right)^{r_{13;2}} (-\log u_{1|2})^{1-r_{13;2}} = O \left((-\log \alpha)^{r_{13;2}} (-\log u_2)^{1-r_{13;2}} \right).$$

According to (C.7),

$$C_{3|2}(v|u_2) \sim \left(1 + \left(\frac{-\log v}{-\log u_2}\right)^{1/r_{23}}\right)^{q_{23}+r_{23}-1} \exp \left(-(-\log u_2) \left(1 + \left(\frac{-\log v}{-\log u_2}\right)^{1/r_{23}}\right)^{r_{23}} + (-\log u_2) \right).$$

For $C_{3|2}(v|u_2) = C_{3|1;2}^{-1}(\alpha|u_{1|2})$ to hold, it has to be true that $(-\log v)/(-\log u_2) \rightarrow 0$ as $u_2 \rightarrow 0$. As a result,

$$-\log C_{3|2}(v|u_2) \sim r_{23} \frac{(-\log v)^{1/r_{23}}}{(-\log u_2)^{1/r_{23}-1}}.$$

Solving for $-\log C_{3|2}(v|u_2) = -\log C_{3|1;2}^{-1}(\alpha|u_{1|2})$, we have

$$-\log v = -\log C_{3|12}^{-1}(\alpha|u_1, u_2) = O\left((-\log \alpha)^{r_{23}r_{13;2}}(-\log u_2)^{1-r_{23}r_{13;2}}\right).$$

On the normal scale, it implies that, with $u_2 = \Phi(x_2) \sim \phi(x_2)/|x_2|$,

$$F_{Y|X_1, X_2}^{-1}(\alpha|x_1, x_2) \sim (-2\log v)^{1/2} = O\left((-\log \alpha)^{r_{23}r_{13;2}/2}|x_2|^{1-r_{23}r_{13;2}}\right), \quad x_1, x_2 \rightarrow -\infty, x_2/x_1 \rightarrow \sqrt{k}.$$

Since $1 - r_{23}r_{13;2} < 1$, the conditional quantile function goes to $-\infty$ sublinearly with respect to x_1 or x_2 .

Upper tail

We give a more detailed analysis to derive the rate at which the conditional quantile goes to $+\infty$. Assume $(1 - u_2) \sim (1 - u_1)^k$ as $(u_1, u_2) \rightarrow (1, 1)$. Let $M_{12}, M_{23}, M_{13;2}$ be the parameters of ψ_{12} for C_{12} , ψ_{23} for C_{23} and $\psi_{13;2}$ for $C_{13;2}$ respectively.

- If $k > 1$, then $u_{1|2} \rightarrow 0$. For a fixed quantile level $\alpha \in (0, 1)$, $u_{3|2}$ has to converge to 0. By (C.13),

$$u_{1|2} \sim (1 - u_2)^{(M_{12}-1)(1/k-1)/M_{12}} \rightarrow 0, \quad -\log u_{1|2} = O(-\log(1 - u_2)).$$

By (C.11), as $u_2 \rightarrow 1$,

$$u_{3|2} \sim \left(1 + \left(\frac{1-v}{1-u_2}\right)^{1/M_{23}}\right)^{M_{23}-1} \sim \left(\frac{1-v}{1-u_2}\right)^{1-1/M_{23}} \rightarrow 0.$$

$$-\log u_{3|2} \sim \left(1 - \frac{1}{M_{23}}\right) (-\log(1-v) + \log(1-u_2)).$$

Since $C_{13;2}$ has $\kappa_{13L} \in (1, 2)$, with a Taylor expansion of (C.7),

$$-\log u_{3|12} \sim r_{13;2} \frac{(-\log u_{3|2})^{1/r_{13;2}}}{(-\log u_{1|2})^{1/r_{13;2}-1}} \sim r_{13;2} \frac{\left(1 - \frac{1}{M_{23}}\right)^{1/r_{13;2}} (-\log(1-v) + \log(1-u_2))^{1/r_{13;2}}}{(-\log(1-u_2))^{1/r_{13;2}-1}}.$$

Let $u_{3|12} = \alpha$ and solve for v , we have

$$-\log(1-v) \sim -\log(1-u_2) + O\left((-\log \alpha)^{r_{13;2}}(-\log(1-u_2))^{1-r_{13;2}}\right) \sim -\log(1-u_2).$$

On the normal scale, it implies

$$F_{Y|X_1, X_2}^{-1}(\alpha|x_1, x_2) \sim x_2, \quad x_1, x_2 \rightarrow +\infty, x_2/x_1 \rightarrow \sqrt{k}.$$

- If $k = 1$, then $u_{1|2} \rightarrow 2^{M_{12}-1}$. For a fixed quantile level $\alpha \in (0, 1)$, $u_{3|2}$ has to converge to a constant. Specifically, $u_{3|2} \rightarrow C_{3|1;2}^{-1}(\alpha|2^{M_{12}-1}) = O(1)$. By (C.11),

$$u_{3|2} \sim \left(1 + \left(\frac{1-v}{1-u_2}\right)^{1/M_{23}}\right)^{M_{23}-1} = O(1),$$

$$1 - v = O(1 - u_2),$$

$$-\log(1-v) \sim -\log(1-u_2).$$

On the normal scale, it implies

$$F_{Y|X_1, X_2}^{-1}(\alpha|x_1, x_2) \sim x_2, \quad x_1, x_2 \rightarrow +\infty, x_2/x_1 \rightarrow 1.$$

- If $k < 1$, then $u_{1|2} \rightarrow 1$. For a fixed quantile level $\alpha \in (0, 1)$, $u_{3|2}$ has to converge to 1. By (C.13),

$$u_{1|2} \sim 1 + (M_{12} - 1)(1 - u_2)^{(1/k-1)/M_{12}} \rightarrow 1,$$

$$\log(1 - u_{1|2}) \sim \frac{1}{M_{12}} \left(\frac{1}{k} - 1 \right) \log(1 - u_2).$$

By (C.11),

$$u_{3|2} \sim \left(1 + \left(\frac{1-v}{1-u_2} \right)^{1/M_{23}} \right)^{M_{23}-1} \sim 1 + (M_{23} - 1) \left(\frac{1-v}{1-u_2} \right)^{1/M_{23}} \rightarrow 1.$$

$$\log(1 - u_{3|2}) \sim \frac{1}{M_{23}} (\log(1 - v) - \log(1 - u_2)).$$

Since $C_{13;2}$ has $\kappa_{13U} = 1$,

$$u_{3|12} \sim \left(1 + \left(\frac{1 - u_{3|2}}{1 - u_{1|2}} \right)^{1/M_{13;2}} \right)^{M_{13;2}-1}.$$

Let $u_{3|12} = \alpha$ and solve for v , we have

$$\left(\alpha^{\frac{1}{M_{13;2}-1}} - 1 \right)^{M_{13;2}} \sim \frac{1 - u_{3|2}}{1 - u_{1|2}},$$

$$\begin{aligned} M_{13;2} \log \left(\alpha^{\frac{1}{M_{13;2}-1}} - 1 \right) &\sim \log(1 - u_{3|2}) - \log(1 - u_{1|2}) \\ &\sim \frac{1}{M_{23}} (\log(1 - v) - \log(1 - u_2)) - \frac{1}{M_{12}} \left(\frac{1}{k} - 1 \right) \log(1 - u_2). \\ &\sim \frac{1}{M_{23}} \log(1 - v) - \left(\frac{1}{M_{23}} + \frac{1}{M_{12}} \left(\frac{1}{k} - 1 \right) \right) \log(1 - u_2). \\ -\log(1 - v) &\sim \left(1 + \frac{M_{23}}{M_{12}} \left(\frac{1}{k} - 1 \right) \right) (-\log(1 - u_2)). \end{aligned}$$

On the normal scale, it implies

$$F_{Y|X_1, X_2}^{-1}(\alpha|x_1, x_2) \sim \sqrt{1 + \frac{M_{23}}{M_{12}} \left(\frac{1}{k} - 1 \right)} x_2, \quad x_1, x_2 \rightarrow +\infty, \quad x_2/x_1 \rightarrow \sqrt{k}.$$

G Additional analysis of the Abalone data set

Figure 11 compares the predicted values on the test set using different models. It indicates that R-vine regression and D-vine regression achieve similar performance; R-vine Gaussian regression and linear regression achieve similar performance. For the other pairs of methods, the predicted values mainly differ on the samples that are near the upper boundary of the covariate space.

The advantage of copula-based models is in modeling the tail behaviors. In order to demonstrate this advantage, we simulate a set of data that are extreme in one or several predictor variables, and perform prediction on this simulated “extreme dataset”. Specifically, we generate samples from the fitted vine copula model and only keep the samples with at least one predictor greater than its corresponding 90% quantile. Figure 12 shows 500 simulated extreme samples overlaying the original data points. Prediction performance of the three fitted models on this extreme dataset is shown in Table 6. It indicates that linear regression cannot properly handle the non-linearity and heteroscedasticity at tails.

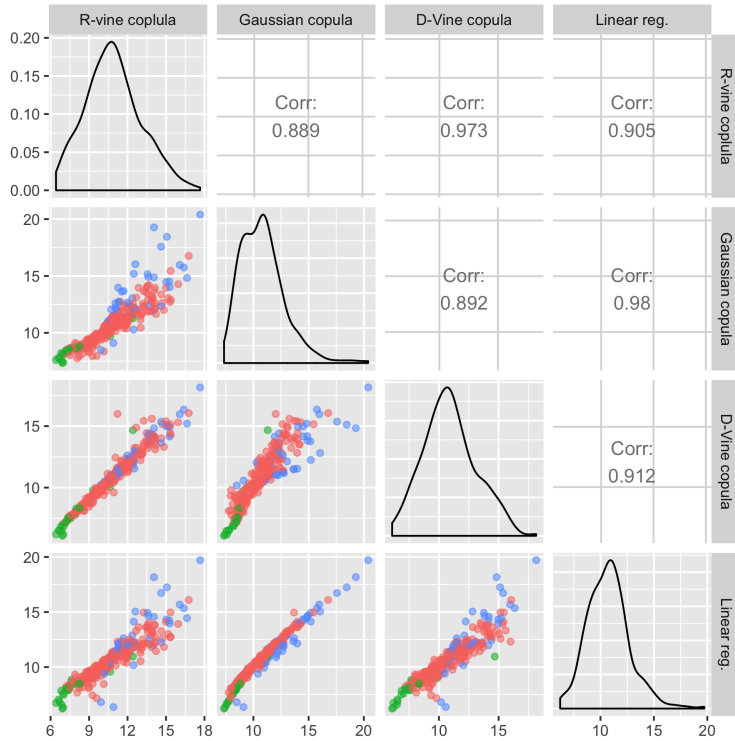


Figure 11: Pair plot of predicted values on the test set using different models. Blue points are samples with at least one explanatory variable above its 95% quantile. Green points are samples with at least one explanatory variable below its 5% quantile. Red points are the other samples. It shows that the predicted values of the methods mainly differ on the samples near the upper boundary of the covariate space.

	R-vine copula	Gaussian copula	D-vine copula	Linear reg.
Root-mean-square error	3.406	3.603	3.439	4.050
Median absolute error	2.415	2.368	2.166	2.619
Mean interval length	10.209	9.210	10.042	8.960
Coverage proportion	0.874	0.808	0.884	0.734
OOSLLK	-2.659	-2.891	-2.644	-3.281

Table 6: Comparison of the performance of vine copula regressions and linear regression on a simulated data set with extreme covariates.

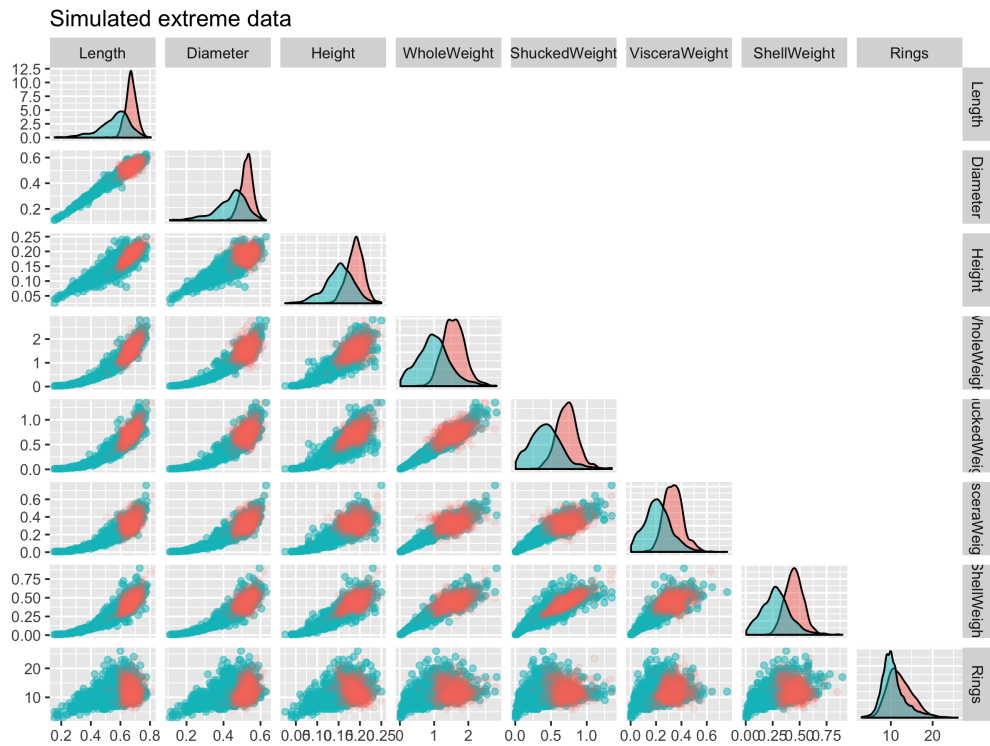


Figure 12: The simulated extreme dataset. The red points are the simulated extreme samples and the cyan points are the original data. It shows that the support of the extreme dataset is approximately a subset of the original data support.